



Cite this: *Mater. Adv.*, 2021, 2, 6816

## A comprehensive review on the environmental applications of graphene–carbon nanotube hybrids: recent progress, challenges and prospects

Jomol P. John, <sup>a</sup> Mary Nancy T. E. <sup>b</sup> and Bindu Sharmila T. K. <sup>\*c</sup>

Environmental pollution by water-soluble pollutants, heavy metal ions and harmful greenhouse gases is triggering significant concern worldwide and is affecting the stability of the environment. Hence, it is indispensable to develop novel materials to mitigate environmental pollution. Graphene/carbon nanotube hybrid materials exhibit exceptional potential for environmental applications including sensing and monitoring of contaminants and their remediation. These 3D network materials possess a larger surface area, enhanced electrical conductivity, thermal conductivity, porosity, minimal agglomeration and higher mechanical strength compared to their building blocks, *i.e.*, 1D carbon nanotubes (CNTs) and 2D graphene. Moreover, the porosity and extremely interconnected structures of these hybrid materials yield an accessible interior surface area, efficient mass transport, etc. These outstanding properties combined with the hydrophobicity, stability and conductivity of these materials provide a general platform for the detection and disposal of various pollutants. This review presents the promising environmental applications of 3D graphene/CNT hybrid materials with special focus on the synergistic effects arising from the combination of graphene and CNT. Most of the relevant literature related to the removal of oils and organic solvents, adsorption of dyes, removal of heavy metal ions, gas sensors and the catalytic conversion of pollutants is reviewed to shed light on the current challenges and upcoming opportunities.

Received 12th April 2021,  
Accepted 6th September 2021

DOI: 10.1039/d1ma00324k

[rsc.li/materials-advances](http://rsc.li/materials-advances)

<sup>a</sup> Department of Chemistry, Maharajas College Ernakulam, 682011, Kerala, India. E-mail: [jomoljohn2001@gmail.com](mailto:jomoljohn2001@gmail.com)

<sup>b</sup> Department of Chemistry, Fatima Mata National College, Kollam, 691001, Kerala, India. E-mail: [marynancy@fmnc.ac.in](mailto:marynancy@fmnc.ac.in)

<sup>c</sup> Department of Chemistry, Maharajas College Ernakulam, 682011, Kerala, India. E-mail: [drbindusharmilatk@maharajas.ac.in](mailto:drbindusharmilatk@maharajas.ac.in); Tel: 9446892578



Jomol P. John

*Jomol P. John began her academic career in 2013 in the Collegiate Education Department and is presently working as an Assistant Professor in Govt. Polytechnic College Perumbavoor, Ernakulam, Kerala, India. She is passionate to learn about the applications of hybrid nanomaterials and is currently doing research in this area under the guidance of Dr Bindu Sharmila T. K., Associate Professor of Chemistry, Maharaja's College Ernakulam. She has more than eight years of experience in academia and research. Her research interests include materials science, nanotechnology and applications of polymer nanocomposites.*



Mary Nancy T. E

*Dr Mary Nancy T. E. is currently working as an Assistant Professor in the PG & Research Department of Chemistry, Fatima Mata National College (Autonomous), Kollam, Kerala, India. Her research interests include the synthesis of graphene-based nanocomposites and their use in electrochemical applications, mainly as biosensors.*



## 1. Introduction

Graphene, a two-dimensional (2D) single layer of  $sp^2$ -hybridized carbon atoms, has attracted remarkable attention due to its unique combination of high surface area, mechanical properties and electrical conductivity.<sup>1–4</sup> However, to minimize the surface free energy, aggregation of the graphene sheets and restacking occur due to their strong van der Waals interactions, thereby greatly hindering the practical applications of graphene.<sup>1</sup> Thus, to overcome this drawback, the surface of the graphene layers must be altered through covalent functionalization, non-covalent stabilization or dispersal in specific solvents.<sup>5</sup>

The high aspect ratio of carbon nanotubes (CNTs) together with their remarkable electrical conductivity, mechanical properties, and most importantly, their similar carbon structure enable them to function as an effective spacer between graphene sheets to create 3D nanostructures having enriched functional properties.<sup>6–8</sup> Fig. 1(a–c) presents images of a 1D CNT, 2D graphene, and 3D graphene–CNT hybrid.

Remarkable research has been conducted in recent years to combine the extraordinary properties of carbon nanotubes and graphene and integrate them to form 3D hybrid systems.<sup>9–12</sup> The integration of CNTs and graphene prevents the re-stacking of graphene sheets and helps to achieve the practical utilization of the synergistic effect between CNTs and graphene. Moreover, CNTs can improve electron transfer by bridging the defects and increasing the layer gap among graphene sheets.

Graphene/CNT hybrid materials possess larger surface area, enhanced electrical conductivity, thermal conductivity, porosity, minimal agglomeration and higher mechanical strength than their building blocks. Moreover, the porosity and extremely interconnected structures of these hybrid materials yield an accessible interior surface area, efficient mass transport, *etc.*<sup>13</sup> Besides being superhydrophobic, they exhibit superoleophilicity, which enables their use as potential materials to remedy oil spills and pollution problems.<sup>14</sup> These 3D hybrid materials

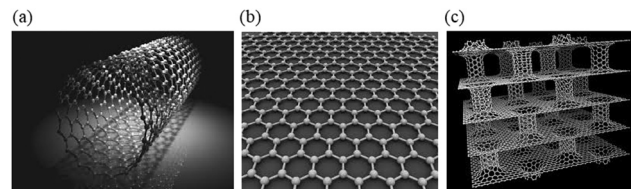


Fig. 1 (a) CNT (1D). (b) Graphene (2D). (c) Graphene–CNT hybrid (3D). Reproduced from ref. 7 with permission from the American Chemical Society.

exhibit excellent electrical properties, which make them suitable for application as electrochemical sensors. The outstanding electrical conductivity of these materials coupled with surface functionalization by various nanoparticles makes them suitable for catalytic applications. Moreover, they possess remarkable mechanical stability, flexibility and strength, which are desirable for various environmental applications.

3D graphene/carbon nanotube networks exhibit exceptional potential in the efficient removal of harmful pollutants from contaminated air and water owing to their following peculiar properties. Firstly, the 3D hybrid structures based on graphene and CNT combine micro-, meso- and macro-pores, where the micro- and mesoporosity provide a high surface area while their macroporosity guarantees accessibility to this surface, enabling the diffusion and transfer of contaminant molecules and ions.<sup>11</sup> Secondly, these 3D hybrids are highly stable, and thus can be applied in various environments including severe acidic conditions<sup>15</sup> and a wide temperature range.<sup>16</sup> Thirdly, their integrated morphology offers effective contaminant separation and recycling and minimizes possible environmental risks triggered by the accidental release of graphene and CNT.<sup>17</sup>

Depending on their architecture, graphene/CNT hybrids can be categorised into (i) hybrids of graphene with vertical CNTs (G/vCNT), (ii) hybrids of graphene with horizontal CNTs (G/hCNT) and (iii) CNTs wrapped with graphene (G/wCNT).<sup>10,18–21</sup> There are two fundamentally different approaches for the synthesis of these hybrids, which are the assembly method and *in situ* method.

The assembly method employs various methods such as layer-by-layer assembly, sol-gel synthesis, vacuum filtration, solution processing, and electrophoretic deposition.<sup>10,22,23</sup> Because of their simplicity and scalability, these methods are extensively employed to assemble G/hCNT and G/wCNT hybrids through non-covalent interactions such as electrostatic,  $\pi$ – $\pi$  stacking, van der Waals and covalent interactions between the functional groups of graphene and CNTs. However, the assembly processes has some significant limitations such as multi-step processing as well as poor control of the orientation, density and morphology of the hybrid structures.

The *in situ* growth of graphene/CNT hybrids can result in better control of the nanoscale architecture than assembly-based methods by adjusting the fabrication conditions. *In situ* approaches (chemical unzipping, chemical vapor deposition, *etc.*) guarantee a uniform distribution of carbon allotropes and



Bindu Sharmila T. K

*Dr Bindu Sharmila T. K. is a Doctoral Degree holder in Chemistry who is enthusiastic in the research of hybrid nanomaterials. She has more than fifteen years of experience in academia and research. She has published papers in refereed international journals of repute. Her research interests include polymer nanocomposites, nanotechnology and materials science. She is a recognized research guide in Chemistry of Mahatma Gandhi University and presented many research papers in international and national conferences. She started her academic career in 2006 at Collegiate Education and has been working as an Associate Professor in the Department of Chemistry, Maharaja's College Ernakulam since 2015.*

*research papers in international and national conferences. She started her academic career in 2006 at Collegiate Education and has been working as an Associate Professor in the Department of Chemistry, Maharaja's College Ernakulam since 2015.*



involve less processing steps.<sup>6,24,25</sup> Covalently bonded seamless hybrid structures of G/hCNT, G/vCNT and G/wCNT are produced by these methods.<sup>25–27</sup> However, for industrial scale production, the use of toxic chemicals (Ni (CO)<sub>4</sub>, B<sub>2</sub>H<sub>6</sub>, *etc.*), explosives and high processing temperature limit their practical application, and hence requires further improvements.

Although the synthesis, properties and applications of 3D graphene/CNT hybrids have been reviewed earlier,<sup>11–13,28,29</sup> the numerous studies on the applications of these materials in recent years make it necessary to recap the advances in this area. Considering that studies on the environmental applications of 3D graphene/CNT hybrids are crucial for our survival, the present review aims to present promising environmental applications related to the removal of oils and organic solvents, adsorption of dyes, removal of heavy metal ions, gas sensing and the catalytic conversion of pollutants to shed light on the current challenges and upcoming opportunities.

## 2. Removal of oils and organic solvents

Accidental spills of catastrophic oils and chemical reagents during extraction, storage and transportation cause adverse impacts on the marine and land ecosystems and impose a series of issues related to environmental pollution.<sup>30–32</sup> Moreover, oil spills lead to loss of energy resources.<sup>33</sup> Hence, it is inevitable to develop efficient remediation methods. To address this severe issue, various techniques including membrane filtration, biological separation, photo decomposition, use of chemical dispersants and skimmers, combustion, wet oxidation and adsorption have been recommended.<sup>34–36</sup> Among them, adsorption is considered the most efficient, economical and promising solution due to its low cost, easy operation, simple process and little damage to the environment.<sup>31,37</sup> However, although several sorbent materials such as fibres,<sup>38</sup> cross-linked polymers and resins,<sup>39,40</sup> polymer gels,<sup>41,42</sup> organic–inorganic hybrids,<sup>43</sup> silica,<sup>44</sup> carbon-based materials<sup>45</sup> and nanocomposites<sup>46</sup> have been established, these materials exhibit certain drawbacks. For example, microporous polymers exhibit high adsorption capacity but their production cost is high. Moreover, even though expanded graphite can efficiently remove crude oil and petroleum products, it cannot be applied for several polar solvents such as toluene and dimethyl sulfoxide. Hence, the development of innovative adsorption materials for the efficient separation of organic solvents and oils from water is of increasing significance.

Generally, an efficient oil adsorbent should be highly oil–water selective, *i.e.*, possess high adsorption capacity for oil and strong hydrophobicity, eco-friendly and reusable.<sup>47</sup> Extensive research has been done on the development of innovative porous adsorbents having superhydrophobicity and superoleophilicity. In this regard, allotropes of carbon such as CNTs and graphene have emerged as potential materials to deal with oil spill and pollution problems by exploiting their hydrophobic interfacial properties.<sup>48–51</sup>

Various sorbents remove or retrieve contaminants either by absorption or adsorption, or both. Absorption occurs *via* the

intermolecular penetration of oil into the pores of the sorbent, and hence depends on the porosity of sorbents together with the viscosity and adhesion properties of oil. During adsorption, oil is accumulated or retained on the surface.<sup>52</sup> In contrast, the driving force leading to adsorption is the attraction between oil and the outer surface of the sorbents, which is controlled by various physical and chemical interactions such as hydrogen bonding, van der Waals forces, steric interactions, hydrophobicity, and polarity.<sup>53</sup>

CNT sponges made up of self-assembled interconnected CNT networks with an expected porosity of >99% were synthesised by Gui *et al.*, which could be utilised more than thousand times without substantial changes in their structure, absorption capacity and hydrophobicity. The sponges had excellent structural flexibility (Fig. 2a) and huge strain deformation with nearly full volume recovery. They exhibited a contact angle of about 156° for water droplets, and owing to their low density, could float on water.<sup>50</sup> For various oils and solvents, they exhibited high absorption capacities ranging from 80 to 180 times their weight. Vegetable oil absorption by a CNT sponge in a water–oil mixture is presented in Fig. 2b. The high absorption capability and rapid absorption were because of the physisorption of molecules and ability to store them in sponge pores. By utilizing mechanical compression, the absorbed oil or solvent molecules could be recovered.

Graphene-based macrostructures also show excellent applications for the removal of organic solvents and oil because of their vast surface area, ultra-lightness, abundant porosity, hydrophobic nature, ability of surface functionalization and high compressibility.<sup>54,55</sup> Moreover, they are more cost effective than CNTs. Aromatic solvents generally exhibit greater affinity for these sorbents compared to aliphatic solvents because of their strong stacking interactions.<sup>56</sup>

To prepare graphene sheets from graphite, one of the frequently used routes is *via* graphite oxide. The underlying basic strategy is to completely exfoliate graphite oxide into individual sheets (graphene oxide), followed by their reduction to produce ‘graphene-like sheets’.<sup>57,58</sup> Graphene oxide (GO), having a high density of functional groups such as hydroxyl and epoxide groups on its basal planes, in addition to carboxyl and carbonyl groups located presumably at the edges, is considered a potential precursor of graphene.<sup>59–64</sup> Although graphene in its oxidized form is nonconductive and sensitive to high temperature, reduced graphene oxide (rGO) can restore these properties.<sup>65,66</sup> However, it is difficult to fully restore the structure and properties to that of pristine graphene.

Bi *et al.* prepared spongy graphene *via* the reduction of graphene oxide platelets in a suspension followed by shaping *via* moulding. The macroporous and shape-mouldable material having a density of  $12 \pm 5 \text{ mg cm}^{-3}$  with a specific surface area of  $\sim 432 \text{ m}^2 \text{ g}^{-1}$  could remove various petroleum products and toxic organic solvents at 20 to 86 times its weight (chloroform: 86.1, lubricating oil: 68.5 and toluene: 54.8).<sup>48</sup> For dodecane absorption, it exhibited an absorption rate of  $0.57 \text{ g g}^{-1} \text{ s}^{-1}$ . Interestingly, it could be regenerated more than 10 times through distillation, with a negligible reduction in its oil or



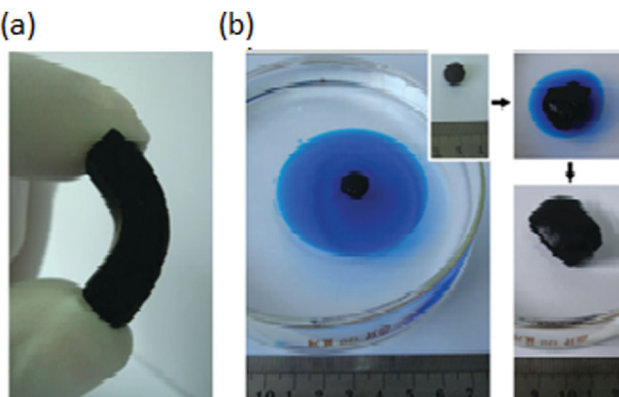


Fig. 2 (a) CNT sponge bent at a large angle. (b) Vegetable oil absorption by CNT sponge. Reproduced from ref. 50 with permission from John Wiley and Sons.

organic sorption capacity, and hence can be employed as a competent recyclable sorbent material (Fig. 3).

In an inspiring work, Zhao *et al.* synthesised a nitrogen-doped 3D graphene framework, which could adsorb organic solvents and oils up to 200–600 times its own weight, *via* the hydrothermal reaction of graphene oxide using pyrrole.<sup>67</sup> The rich open porous structures offered an ultralow density ( $2.1 \pm 0.3 \text{ mg cm}^{-3}$ ) (Fig. 4a). Their adsorption efficiency considering weight gain and comparison of the adsorption capacities of common carbon-based materials are shown in Fig. 4b and c, respectively. They exhibited an adsorption rate ( $41.7 \text{ g g}^{-1} \text{ s}^{-1}$ ) that is higher than that of pure graphene.

Despite the hydrophobicity in graphene-based macrostructures, their high cavity content together with appropriate pore size lead to some water adsorption.<sup>68</sup> In this context, the synthesis of graphene/carbon nanotube hybrids exhibits promising potential. Carbon nanotubes can be utilised to enhance the robustness and surface roughness of graphene, which is attributed to its better adsorption capacity and hydrophobicity. Superoleophilic and super hydrophobic foam of a graphene/CNT hybrid was synthesised

*via* the chemical vapour deposition method in two steps, which exhibited excellent hydrophobic properties due to its surface roughness, bulk porous structure and hydrophobicity of CNTs.<sup>14</sup> This hybrid material can be employed for the elimination of organic solvents and oil in water owing to its macroporous structure and superoleophilicity.

Good efficiency was obtained by an ultra-flyweight aerogel fabricated using CNTs and giant graphene oxide sheets with a very low density ( $0.75 \text{ mg cm}^{-3}$ ). The aerogel obtained was highly hydrophobic, having a contact angle of  $\sim 132.9^\circ$  and surface area of  $\sim 272 \text{ m}^2 \text{ g}^{-1}$  with average pore size of 123 nm. The high porosity of the aerogel ( $\sim 99.9\%$ ) led to the fast and efficient removal of oils, ranging between 215–913 times its weight depending on the oil density. The rate of absorption exhibited by the aerogel ( $68.8 \text{ g g}^{-1} \text{ s}^{-1}$ ) was much greater than that of a graphene aerogel ( $0.57 \text{ g g}^{-1} \text{ s}^{-1}$ ).<sup>69</sup>

Kabiri and co-workers reported a single-step approach for the synthesis of 3-D graphene/CNT networks by heating an aqueous mixture of graphene oxide and CNTs in the presence of  $\text{Fe}^{2+}$  ions.<sup>70</sup> The as-prepared aerogels exhibited exceptional adsorption characteristics for the removal of organic solvents, oils and fats in a non-turbulent water–oil system. The entire oil was instantly adsorbed and entirely taken up within 20 s by immersing the graphene–CNT aerogels in the oil. The oil-filled aerogels could float on the surface of water without releasing the oil or penetration of water into their structure. The graphene–CNT aerogels exhibited an adsorption capacity of 21–35 times its own weight. Compared to other adsorbents tested previously (for gasoline adsorption), such as carbon nanofiber (CNF)/carbon foam ( $16 \text{ g g}^{-1}$ ),<sup>71</sup> CNT–polydimethylsiloxane-coated polyurethane ( $17.5 \text{ g g}^{-1}$ ),<sup>72</sup> cotton grass ( $19 \text{ g g}^{-1}$ )<sup>73</sup> and carbonized pith bagasse ( $23.86 \text{ g g}^{-1}$ ),<sup>74</sup> the graphene–CNT aerogel exhibited a better adsorption performance of  $30 \text{ g g}^{-1}$ . Moreover, its adsorption capacity was enhanced with an increase in the density of the organic solvents and oil. This is because liquids having a higher surface tension and viscosity will repel molecular disruption and also avoid diffusion towards the porous aerogel

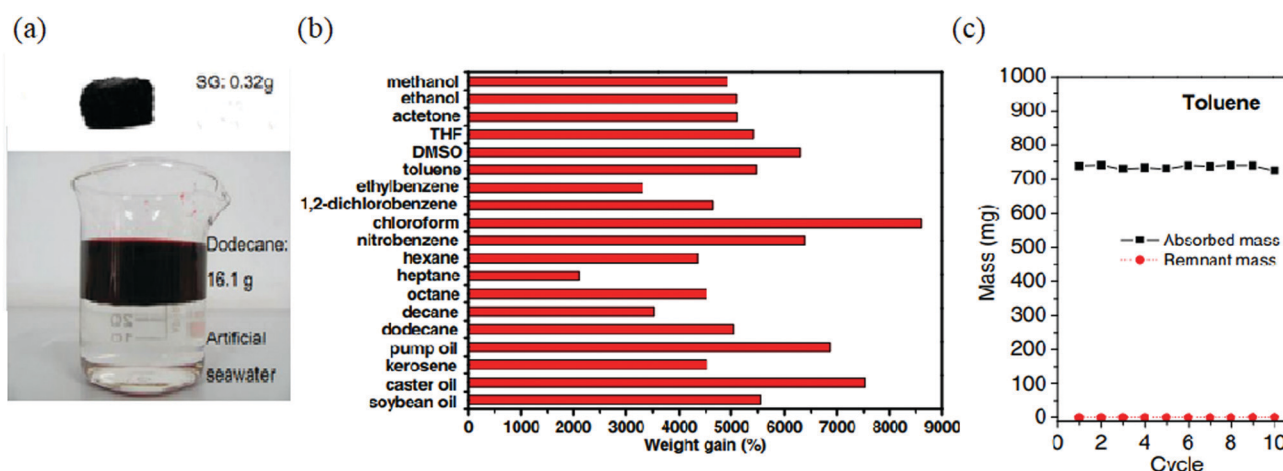


Fig. 3 (a) 0.32 g spongy graphene can remove 16.1 g of dodecane. (b) Sorption efficiency for various oils and organic solvents. (c) Recyclability for 10 cycles. Reproduced from ref. 48 with permission from John Wiley and Sons.

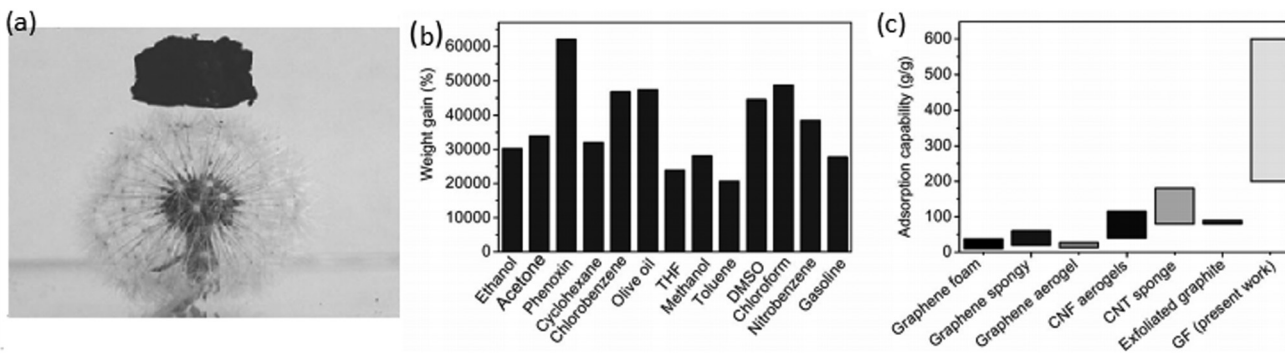


Fig. 4 (a) Piece of GF size of  $1.8\text{ cm} \times 1.1\text{ cm} \times 1.2\text{ cm}$  standing on a dandelion. (b) Adsorption efficiency considering weight gain. (c) Comparison of the adsorption capacities of common carbon-based materials. Reproduced from ref. 67 with permission from John Wiley and Sons.

given that surface molecules attempt to close pack together. It was also reported that the graphene/CNT aerogel could continuously remove organic pollutants and oil in an aqueous system *via* pressure-driven adsorption. Only 350 mg of the graphene/CNT aerogel could separate about 10 L of oil in combination with a vacuum system. Thus, the hybrid aerogel can act as a superior filter for the removal of oil, even after saturation.

Wan *et al.* reported a green and facile method to synthesize graphene/CNT aerogels having a very low density ( $6.2\text{--}12.8\text{ mg cm}^{-3}$ ) *via* a single-step hydrothermal redox reaction. With an enhanced GO/CNT mass proportion (7:1 and 3:1), the adsorption capacities reached 100–270 times their weight depending on the density of the adsorbed organics. Moreover, the graphene/CNT aerogels retained excellent stability and reusability after continuous adsorption-squeezing experiments.<sup>75</sup>

More interestingly, a hydrothermal process to synthesize a graphene aerogel starting with graphene oxide was reported, which was utilized as a template for growing CNTs.<sup>76</sup> The *in situ*-grown CNTs on graphene sheets provided a hierarchical hybrid structure having a low density, exceptional hydrophobicity and oleophilicity together with improved surface area possessing meso- and micro-scale pores. Thus, the hybrid structure exhibited greater adsorption capacity than reduced graphene oxide itself. The material displayed a steady adsorption capacity throughout repeated adsorption/burn operations and retained more than 90% adsorption capacity over 10 cycles (Fig. 5a and b). The adsorption capacity exhibited by the hybrid aerogel for various organic liquids is shown in Fig. 5c with a maximum capacity of  $322.8 \pm 8.3\text{ g g}^{-1}$  for *ortho*-dichlorobenzene. Hence, it can adsorb various oils with excellent reusability. By employing *in situ* burning, the adsorbed solvents were removed easily, while the aerogel retained its porous framework without being burnt in air or collapsing, indicating the outstanding fire resistance and thermal stability of the rGO/CNT aerogel (Fig. 5d).

Physical adsorption can also be employed as an eco-friendly and efficient route for removing organic contaminants from water. Zhan and co-workers introduced 1D poly-dopamine-functionalized multiwalled carbon nanotubes in a graphene aerogel to prepare a robust and ultra-lightweight composite aerogel for the effective adsorption of organic pollutants.<sup>77</sup> Environmental pollution was greatly reduced by using this

composite, as no reducing agents were used for its formation. The surface area and stability of the composite were significantly enhanced after combining with multi-walled carbon nanotubes (MWCNTs). The reduction in pore size improved the capillary flow and absorption for organic contaminants, ranging from 125 to  $533\text{ g g}^{-1}$ , which exceeded that of most of reported absorption materials. Moreover, the composite displayed an outstanding reusable performance in absorption-combustion, absorption-distillation and absorption-squeezing cycles depending on the characteristics of the various organic solvents.

In another interesting study, fluffy spheres of CNTs/graphene/nickel were developed by employing renewable carbon sources.<sup>78</sup> Carbon-encapsulated nickel nanoparticles were prepared through the hydrothermal carbonization of potato starch at a low temperature and catalytically graphitized and cracked in biogas at  $700\text{ }^{\circ}\text{C}$ . The graphene shells were peeled off to form graphene nanoplatelets and MWCNTs grew and *in situ* integrated into the platelets. For the removal of organic solvents from water, the prepared nanocomposite showed an exceptional performance with an adsorption capacity ranging from  $\sim 112$  to  $\sim 145\text{ g g}^{-1}$ .

Cai *et al.* reported the synthesis of an aerogel, rGO/amino MWCNT, through the chemical reaction between the  $-\text{COOH}$  groups on GO and  $-\text{NH}_2$  groups on amino MWCNT in combination with a freeze-drying and high-temperature annealing process.<sup>79</sup> The presence of strong chemical bonding enhanced the hydrophobic property and microstructures of the hybrid aerogel. Oil-water separation experiments and adsorption tests proved the outstanding adsorption capability of the aerogel for various oils and organic solvents such as dichloromethane ( $242.31\text{ g g}^{-1}$ ), acetone ( $219.54\text{ g g}^{-1}$ ), sesame oil ( $156.35\text{ g g}^{-1}$ ), ethyl acetate ( $152.79\text{ g g}^{-1}$ ) and cyclohexane ( $122.46\text{ g g}^{-1}$ ). Moreover, oil-water separation was achieved within 25 s.

Decorating graphene/CNT-based sorbents using magnetic nanoparticles facilitates their easy collection after saturation using a magnetic field. Moreover, they can be employed to 'mop-up' oil on the surface of water with the help of a permanent magnet to move them around to track oil spills.<sup>80</sup> Even if the sorbent is accidentally smashed, all the broken pieces of sorbent can be safely recovered. Based on their facile synthetic methods, high adsorption capability, stable cyclic



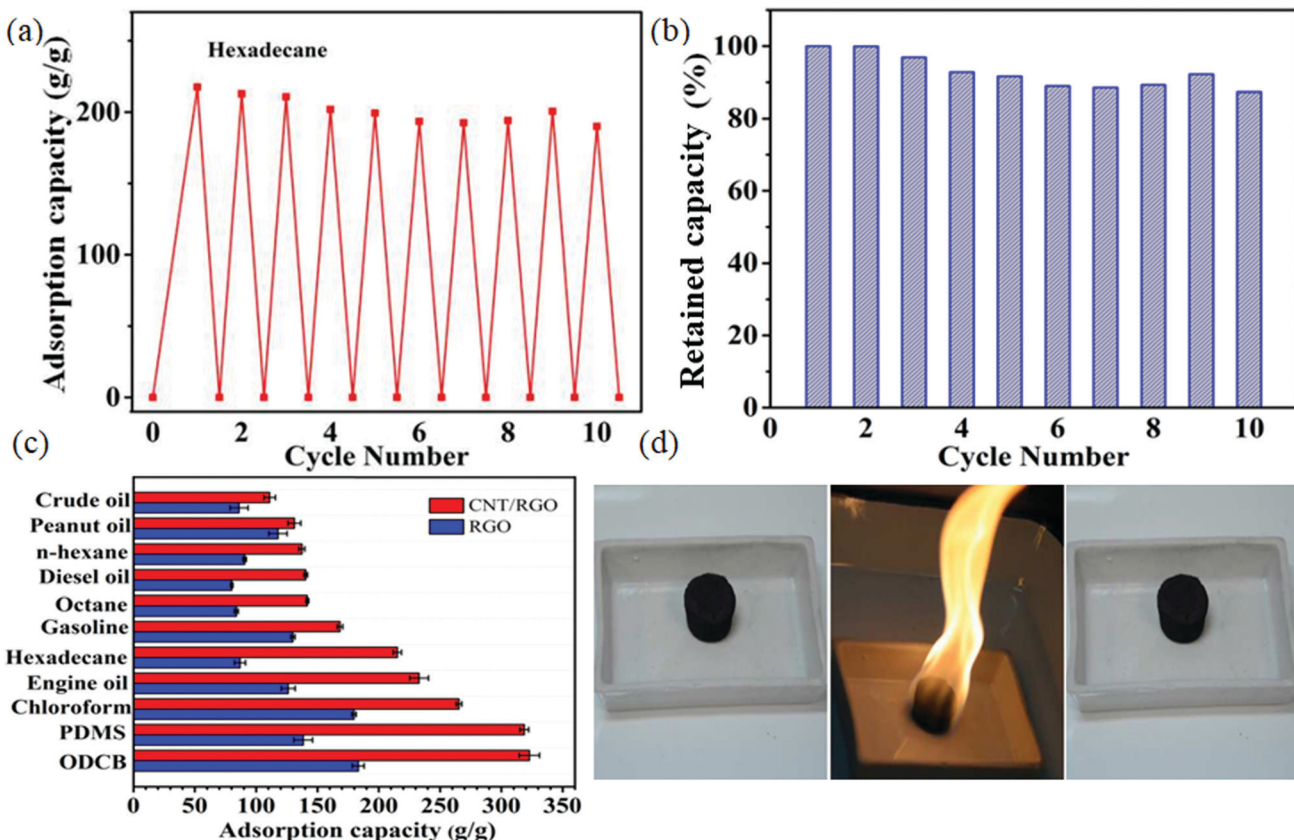


Fig. 5 (a) Adsorption recyclability of hybrid aerogel over ten cycles. (b) Retained adsorption capacity exhibited by the sample. (c) Adsorption capacity of hybrid aerogel for different organic liquids. (d) Outstanding thermal stability, and hence reusability of hybrid aerogel via combustion. Reproduced from ref. 76 with permission from Elsevier.

performance, *etc.*, graphene–CNT hybrid structures show huge potential in water decontamination and oil remediation. The performance of graphene–CNT hybrids for the removal of various oils and organic solvents is summarized in Table 1. Further research to control the functional groups on graphene surface to couple selective adsorption characteristics and achieve the highest hydrophobicity is essential in this area.

### 3. Adsorption of dyes

With the rapid industrial development, water pollution resulting from organic dyes discharged from the textile, leather, food, plastic, paper, cosmetics and pharmaceutical industries without adequate treatment processes has become a serious problem affecting aquatic life, human health and the ecosystem because of their colour and high chemical oxygen demand.<sup>81,82</sup> The release of exceedingly coloured waste interferes with the transmission of light, and thus upsets biological processes, causing harm to aquatic systems. Many organic dyes exhibit resistance to bio-degradation. Moreover, they are stable to light, chemical treatments *etc.*, and thus result in high bio-toxicity and carcinogenic effects. Therefore, the development of innovative treatment processes for the efficient removal of dyestuffs has attained great importance and special interest.<sup>83</sup> Most dyes are

dissolved in cationic (Rhodamine B, methylene blue, malachite green, *etc.*) or anionic (Bordeaux red, methyl orange, rose Bengal sodium salt, *etc.*) forms. Thus, the rich porous structure and vast surface area of graphene/CNT hybrids allow the diffusion and provide storage space for dye molecules. Moreover, electrostatic and efficient  $\pi$ – $\pi$  interactions can be exploited to take full advantage of these materials for the effective adsorption of dyes, particularly those having aromatic structures.

In this regard, an graphene/CNT hybrid aerogel obtained *via* the supercritical  $\text{CO}_2$  drying of its aqueous gel precursors was reported.<sup>84</sup> The ultralight hybrid aerogel exhibited high conductivity ( $7.5 \text{ S m}^{-1}$ ), ample pore volume ( $2.58 \text{ cm}^3 \text{ g}^{-1}$ ), large surface area ( $435 \text{ m}^2 \text{ g}^{-1}$ ) and excellent scavenging ability for basic dyes as a sorbent. It exhibited an adsorption capacity of  $145.9 \text{ mg g}^{-1}$  for Rhodamine B, which is higher than that with substances such as *Rhizopus oryzae* biomass ( $39.08 \text{ mg g}^{-1}$ ), *O*-carboxymethyl chitosan-*N*-lauryl ( $38.5 \text{ mg g}^{-1}$ )<sup>85</sup> and porous graphitic carbon ( $73.0 \text{ mg g}^{-1}$ )<sup>86</sup> for the same dye. The acid-treated MWCNT/graphene hybrid aerogel exhibited an adsorption capacity of  $190.9 \text{ mg g}^{-1}$  for methylene blue, which is much higher than that with most of the conventional adsorbents under similar conditions for the same dye.<sup>87</sup> For the adsorption of acid fuchsin, the MWCNT/graphene and acid-treated MWCNT/graphene hybrid aerogels exhibited an adsorption capacity of  $66.4 \text{ mg g}^{-1}$  and  $35.8 \text{ mg g}^{-1}$ , respectively (Fig. 6).



Table 1 Performance of graphene–CNT hybrids for the removal of various oils and organic solvents

Sl No.	Type of material	Synthetic method	Target	Removal capacity (g g <sup>-1</sup> )	Ref.
1	CNT sponge	CVD using 1,2-dichlorobenzene and ferrocene	Various oils and organic solvents	80–180	50
2	Spongy graphene	Reducing graphene oxide platelets in suspension followed by shaping <i>via</i> moulding	Petroleum products, fats, toluene, alkanes, and other organic solvents	20–86	48
3	Nitrogen-doped 3D graphene	Hydrothermal reaction of graphene oxide using pyrrole	Various oils and organic solvents	200–600	67
4	Graphene/CNT hybrid foam	Two-step CVD including CNT growth on graphene–Ni substrate followed by removal of Ni	Compressor oil, sesame oil, toluene, chloroform, dimethylformamide, etc.	80–130	14
5	Graphene/CNT aerogel	Freeze drying aqueous solutions of graphene oxide sheets and CNTs followed by reduction	Crude oil, motor oil, vegetable oil, <i>n</i> -hexane, 215–913 ethanol, toluene, 1,4-dioxane, chloroform, etc.	215–913	69
6	Graphene/CNT aerogel	Reduction of graphene oxide in presence of Fe nanoparticles and formation of graphene–CNT hydrogel followed by freeze drying	Various oils (gasoline), fats (vegetable oils and paraffin) and organic solvents (toluene and tetrahydrofuran)	21–35	70
7	Graphene–CNT aerogel	Hydrothermal redox reaction involving the addition of ethylenediamine to graphene oxide–CNT dispersion followed by heating and freeze drying	Various oils and organic solvents including <i>n</i> -hexane, toluene, phenixin and lube	100–270	75
8	Graphene–CNT aerogel	Preparation of graphene aerogel using GO <i>via</i> a hydrothermal process followed by <i>in situ</i> growth of CNTs	Petroleum products, chloroform, hexane, octane, peanut oil, <i>ortho</i> -chlorobenzene, etc.	110–330	76
9	Graphene/MWCNT–PDA composite aerogel	Preparation of GO/MWCNT-PDA hydrogel followed by freeze drying and annealing	Acetone, chloroform, <i>n</i> -dodecane, <i>n</i> -hexane and <i>n</i> -heptane	125–533	77
10	CNTs/graphene/Ni fluffy spheres	Catalytical graphitization of carbon encapsulated Ni nanoparticles followed by cracking and <i>in situ</i> growth of MWCNT into the graphene nanoplatelets	Various oils and organic solvents–hexane, gasoline, chloroform, diesel, toluene and dichlorobenzene	112–145	78
11	rGO/amino MWCNT aerogel	Reaction between GO and amino MWCNT together with freeze-drying and annealing	Ethyl acetate, cyclohexane, dichloromethane, acetone and sesame oil	122–242	79

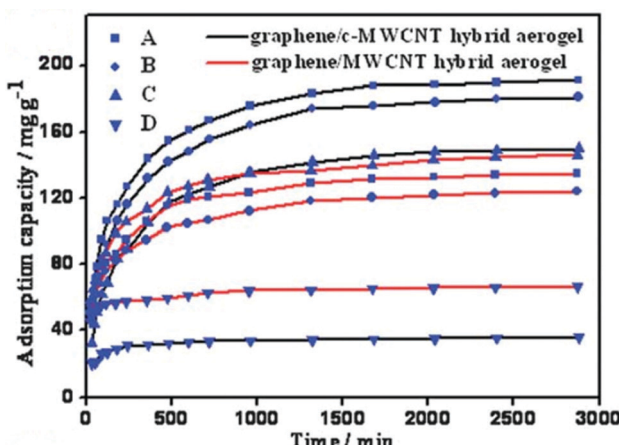


Fig. 6 Adsorption of dyes: methylene blue (A), fuchsin (B), Rhodamine B (C), and acid fuchsin (D) by graphene/MWCNT hybrid aerogel. Reproduced from ref. 84 with permission from The Royal Society of Chemistry.

The electrostatic repulsion between the adsorbed acidic dyes and hybrid aerogels caused relatively lower capacities.

In an interesting work by Ai and Jiang, a graphene–CNT aerogel exhibited an outstanding performance in removing methylene blue from an aqueous solution with a maximum adsorption capacity of 81.97 mg g<sup>-1</sup>. The removal efficiency was 97% at the initial MB concentration of 10 mg L<sup>-1</sup>.<sup>88</sup> Kotal and Bhowmick reported that hybrid materials based on CNT chemically bonded to reduced graphene oxide exhibited a maximum adsorption capacity of 245 mg g<sup>-1</sup> for crystal

violet (greater than that using magnetic-modified MWCNT (228 mg g<sup>-1</sup>) and 219 mg g<sup>-1</sup> for Rhodamine 6G (greater than using cane sugar-reduced graphene (55 mg g<sup>-1</sup>)).<sup>89</sup>

With the progress in adsorption research on graphene/CNT hybrid structures, there have been constant efforts to develop all-carbon nanoarchitecture membranes having improved membrane selectivity and superior water permeability. By intercalating surface-functionalized multi-walled carbon nanotubes with a small diameter into rGO sheets, Goh *et al.* developed exceptionally stable membranes, which could reject almost 100% organic dyes having different charges (cationic: Rhodamine B and methylene blue and anionic: Acid Orange 7). The exceptional stability exhibited by these materials resulted from the van der Waals force and  $\pi$ – $\pi$  interactions between the rGO sheets and MWCNTs. Moreover, their water permeability of 52.7 L m<sup>-2</sup> h<sup>-1</sup> bar<sup>-1</sup> was 4.8 times that of pristine rGO membrane and 5–10 times greater than that most commercial nanofiltration membranes.<sup>90</sup>

Lee *et al.* synthesised a hybrid graphene–CNT aerogel by growing CNTs on the surface of a graphene aerogel using a nickel catalyst.<sup>91</sup> The large specific surface area together with mesoporous nature of the hybrid material made it suitable for water treatment. The hybrid aerogel obtained *via* the chemical vapour deposition of CNTs on graphene metal salts (G-CNT\_A) exhibited a superior adsorption capacity for methylene blue of 626 mg g<sup>-1</sup>. Van der Waals forces together with the  $\pi$ – $\pi$  interaction among the nanocarbon materials and organic dyes resulted in high adsorption. It could effectively remove anionic and cationic dyes from water. The adsorption capacity of G-CNT\_A for methyl orange was 532 mg g<sup>-1</sup> and Congo red

was 560 mg g<sup>-1</sup>, which was much greater compared to that of other graphene-based adsorbents (methyl orange: 101.34 mg g<sup>-1</sup><sup>92</sup> and Congo red: 33.66 mg g<sup>-1</sup><sup>93</sup>). The adsorption capacity for crystal violet of 575 mg g<sup>-1</sup> was greater than that obtained with the hybrid material based on CNT chemically bonded to reduced graphene oxide (245 mg g<sup>-1</sup>). Moreover, owing to its magnetic nature, the aerogel was easy to separate from water and could be readily recycled and reused.

Chen *et al.* reported a promising nanofiltration membrane prepared by loading rGO intercalated with CNTs on an anodic aluminium oxide microfiltration membrane using a facile vacuum-assisted filtration method. The membrane was used to separate dyes, nanoparticles, organophosphates, sugars, proteins, and especially humic acid from water. It had good permeability, good anti-fouling properties and high retention efficiency. The retention was greater than 97.3% for methyl orange and the permeability of the membrane was 20–30 L m<sup>-2</sup> h<sup>-1</sup> bar<sup>-1</sup>.<sup>94</sup> Ansari and co-workers employed an oxidative polymerisation technique to combine MWCNT-GO composites with polyaniline, and to generate additional functionality, doped them with *p*-toluene sulfonic acid.<sup>95</sup> The composite was successfully employed for the adsorptive removal of Congo red dye and Cr<sup>4+</sup>, and the maximum adsorption of Congo red dye and Cr<sup>4+</sup> was observed at 30 °C in acidic medium. The highly functionalised nanocomposite system enabled the removal of multicomponent pollutants from aqueous solutions.

Huang *et al.* dispersed GO and modified CNTs (MCNTs) in water, mixed them with toluene, and then porous graphene-CNTs composites were synthesised *via* hydrothermal reaction.<sup>96</sup> By varying the ratio of GO/MCNTs to toluene, the pore size of the composite could be controlled. With a decrease in pore size, the equilibrium adsorption capacity increased and the rate of adsorption decreased. The nanocomposite could maintain good adsorption capacity for methylene blue even after 5 cycles.

Electrochemically enhanced adsorption (electro sorption) can be effectively applied for the superior removal of organic pollutants. For the electrosorption of organic dyes, Yue *et al.* developed a freestanding porous rGO/SWCNT film as a flexible electrode material by assembling SWCNTs and spherical polystyrene into a graphene film, and subsequent reduction and calcination at 500 °C in Ar for 1 h.<sup>97</sup> The 3D porous structure and highly crumpled surface enhanced the diffusion of ions and adsorption. For methylene blue, the film exhibited outstanding recyclability with observed maximum adsorption capacity of 13.01 g g<sup>-1</sup> and the capacity retention after the 5th cycle was ~103%.

$\alpha$ -FeOOH anchored by a GO-CNT aerogel nanocomposite was fabricated *via* a hydrolysis process and employed as a persulfate activator ( $\alpha$ -FeOOH@GCA + K<sub>2</sub>S<sub>2</sub>O<sub>8</sub>) for the decolourisation of Orange II. The decolourisation of the dye was enhanced to ~99% compared to that of the pristine  $\alpha$ -FeOOH (~44%) or GO-CNTs (~18%). The enhanced catalytic activity resulted from the formation of a heterojunction by GO-CNTs and  $\alpha$ -FeOOH, as confirmed by the presence of Fe–O–C bonds. In the case of recycling, the decolourisation efficiency of the dye by the

activated persulfate system dropped from the first to third cycle. However, the addition of a small amount of Fe<sup>2+</sup> or ultraviolet irradiation could restore the activity of the system.<sup>98</sup>

Yao *et al.* fabricated highly porous graphene/carbon nanotube hybrid beads possessing high mechanical strength through the self-assembly of graphene and CNTs together with a poly-acrylonitrile coating and KOH-activated carbonization.<sup>99</sup> The hybrid beads possessed a high specific surface area of 1270 m<sup>2</sup> g<sup>-1</sup>, hierarchical porous structure and low density of 5.7 mg mL<sup>-1</sup>. Moreover, they exhibited outstanding cyclic resilient property, excellent mechanical stability and the maximum adsorption capacity for methylene blue reached ~521.5 mg g<sup>-1</sup>.

Hu *et al.* reported the preparation of 3D graphene oxide/carbon nanotube nanostructures having a large surface area *via* a freeze-drying method.<sup>100</sup> The prepared nanostructures with GO: CNT = 1:5 had a surface area of 257.6 m<sup>2</sup> g<sup>-1</sup> and could adsorb both anionic (methyl orange) and cationic (Rhodamine B) dyes in aqueous solution. The maximum adsorption capacity for methyl orange of 66.96 mg g<sup>-1</sup> and Rhodamine B of 248.48 mg g<sup>-1</sup> was better than that of modified graphene oxides or CNTs. Hence, the synergistic effect of 1D CNTs on 2D graphene can provide a uniform 3D nano filtration membrane, which results in elevated permeability and separation capability. However, studies regarding the practical separation applications of these hybrid structures are limited, further research to develop smart porous membranes is anticipated to occur in the near future.

## 4. Removal of heavy metal ions

As a consequence of urbanization and rapid industrialization over the past few decades, plenty of toxic metal ions have been discharged from industries such as fertilizer production, mining operations, storage batteries, metal processing plants, metal plating, and alloy industries into the environment without adequate treatment processes.<sup>101–103</sup> These contaminants, which are not biodegradable, easily accumulate and cause toxic effects to ecosystems and public health. For the removal of various metals, several methods such as ion-exchange, membrane filtration, chemical precipitation, electrochemical treatment, advanced oxidation, reverse osmosis and adsorption have been developed.<sup>104,105</sup> Among them, adsorption is widely employed for the removal of metals owing to its high efficiency, simple design, ease of operation, low maintenance cost and capability of metal recovery.

Carbon-based nanocomposites have shown promising adsorption performances towards these pollutants. The adsorption process is driven by (i) electrostatic interactions,<sup>106,107</sup> (ii) ion exchange process<sup>108</sup> and (iii) surface complexation with metal ions.<sup>109,110</sup> In the case of electrostatic interactions, heavy metal cations are attracted by the oxygen functionalities (–OH, –O–, –COOH, etc.) on the surface of the adsorbent, which are negatively charged. For ion exchange, metal cations replace the H<sub>3</sub>O<sup>+</sup> groups present in the adsorption sites. Similar to the adsorption of cationic dyes, the adsorption capacity can be



improved by increasing the pH for both mechanisms. Conversely, it is also essential to prevent a high enough pH for precipitating metal hydroxides.<sup>106</sup> Moreover, the adsorption of metal on graphene is endothermic, an enhanced adsorption capacity can be achieved at a higher temperature.

Hybrid polymer-GO sponges have attracted considerable interest for the removal of metal ions, and in this regard, chitosan-gelatin/GO monoliths with high porosity (>97%) were synthesised using a unidirectional freeze drying method for the adsorption of  $\text{Pb}^{2+}$  and  $\text{Cu}^{2+}$ .<sup>111</sup> The introduction of GO considerably enhanced the porous structure and compressive strength of the hybrid monolith. They exhibited high stability, and hence only a slight reduction in adsorption ability was observed even after recycling several times. Moreover, they are nontoxic and biodegradable.

3D graphene-CNT hybrid networks have been deeply investigated on account of their easy separation and large specific surface area. They exhibit outstanding potential for removing heavy metal ions such as  $\text{Cu}^{2+}$ ,  $\text{Pb}^{2+}$ ,  $\text{As}^{3+}$  and  $\text{U}^{6+}$ . A previously mentioned graphene/CNT hybrid aerogel<sup>84</sup> showed high scavenging ability for heavy metal ions as binding species. The binding capacity exhibited by the acid-treated MWCNT/graphene hybrid aerogel for various metals including  $\text{Pb}^{2+}$  of  $0.51 \text{ mmol g}^{-1}$  ( $104.9 \text{ mg g}^{-1}$ ),  $\text{Hg}^{2+}$  of  $0.46 \text{ mmol g}^{-1}$  ( $93.3 \text{ mg g}^{-1}$ ),  $\text{Ag}^+$  of  $0.59 \text{ mmol g}^{-1}$  ( $64 \text{ mg g}^{-1}$ ) and  $\text{Cu}^{2+}$  of  $0.53 \text{ mmol g}^{-1}$  ( $33.8 \text{ mg g}^{-1}$ ) was much greater than that of the MWCNT/graphene hybrid aerogel for the same metals as follows:  $\text{Pb}^{2+}$ - $0.21 \text{ mmol g}^{-1}$  ( $44.5 \text{ mg g}^{-1}$ ),  $\text{Hg}^{2+}$ - $0.38 \text{ mmol g}^{-1}$  ( $75.6 \text{ mg g}^{-1}$ ),  $\text{Ag}^+$ - $0.43 \text{ mmol g}^{-1}$  ( $46 \text{ mg g}^{-1}$ ) and  $\text{Cu}^{2+}$ - $0.15 \text{ mmol g}^{-1}$  ( $9.8 \text{ mg g}^{-1}$ ), as shown in Fig. 7. This is because electrostatic interaction mainly controls the binding of ions to porous hosts<sup>112</sup> and the acid-treated MWCNT/graphene hybrid aerogel possessed more oxygen-containing groups, which led to the efficient binding of ions.<sup>113,114</sup>

It is also interesting that the incorporation of iron minerals in the graphene/CNT networks has the advantage of preventing the aggregation of the carbon nanostructures. Moreover, the

facile separation of the trapped metals can be easily achieved by exploiting their intrinsic magnetic properties.<sup>115</sup> In this regard, Zhang *et al.* synthesised a graphene-CNT hybrid aerogel *via* the hydrothermal reduction of GO and CNTs with the addition of ferrous ions.<sup>116</sup> Owing to its competent porous structure, it exhibited efficient removal of lead ions of  $232\text{--}451 \text{ mg g}^{-1}$ , which is higher than that of other carbon-based adsorbents, including carbonaceous nanofiber membranes ( $221 \text{ mg g}^{-1}$ ) and pure graphene aerogels ( $374 \text{ mg g}^{-1}$ ). The amount of CNTs and ferrous sulphate used had a significant influence on the metal removal efficiency, and that prepared using 30% CNTs had a higher efficiency among the samples with same amount of ferrous sulphate. Moreover, the mass production of graphene-CNT-iron oxide hybrid structures was achieved *via* a one-pot microwave route, which is highly versatile.<sup>117</sup> Owing to its open porous nanostructures and high aspect ratio, the hybrid material exhibited efficient removal of arsenic from contaminated water (Fig. 8).

To separate and remove  $\text{As}^{3+}$  and  $\text{Pb}^{2+}$  from contaminated water, 3D GO membranes bridged with glutathione-conjugated CNT were developed, which could capture  $\text{As}^{3+}$  (>96%),  $\text{As}^{5+}$  (>92%) and  $\text{Pb}^{2+}$  (>98%).<sup>118</sup> The excellent removal efficiency is attributed to the high affinity of  $\text{As}^{3+}$  and  $\text{Pb}^{2+}$  for glutathione, since they can both bind to glutathione using  $-\text{SH}$ . Moreover, the open pore network of the CNT-bridged GO membrane facilitated the fast diffusion of  $\text{As}^{3+}$ ,  $\text{As}^{5+}$  and  $\text{Pb}^{2+}$  inside the 3D network, which resulted in a high adsorption capacity (Fig. 9a-c). In contrast, only 12% of  $\text{As}^{3+}$ , 9% of  $\text{As}^{5+}$  and 18% of  $\text{Pb}^{2+}$  could be removed using the 3D GO membrane bridged with CNT (without glutathione) (Fig. 9d).

The removal of uranium has gained remarkable attention owing to the radioactive damage it causes to human health and the ecology. Graphene-CNT aerogels exhibited a high efficiency for the removal of  $\text{U}^{6+}$  with a monolayer sorption capacity of  $86.1 \text{ mg g}^{-1}$ .<sup>119</sup> Diethylenetriamine-functionalized CNTs dispersed in GO colloids were synthesised for the selective solid-phase extraction and analysis of trace-level  $\text{Cr}^{3+}$ ,  $\text{Fe}^{3+}$ ,  $\text{Pb}^{2+}$ , and  $\text{Mn}^{2+}$  ions in wastewater.<sup>120</sup> The solid-phase sorbent could achieve maximum static adsorption capacities up to 95% for  $\text{Cr}^{3+}$  ( $5.4 \text{ mg g}^{-1}$ ),  $\text{Fe}^{3+}$  ( $13.8 \text{ mg g}^{-1}$ ),  $\text{Pb}^{2+}$  ( $6.6 \text{ mg g}^{-1}$ ) and  $\text{Mn}^{2+}$  ( $9.5 \text{ mg g}^{-1}$ ) within about 30 min. Moreover, common coexisting ions had no substantial interference on the pre-concentration and separation of these ions at pH 4.

Interestingly, hydrosols of CNTs/GO sealed in dialysis bags showed outstanding efficiency for the elimination of trace  $\text{Gd}^{3+}$  from water, without re-pollution.<sup>121</sup> The hybrids having an  $M_{\text{CNTs}} : M_{\text{GO}}$  ratio ranging from 1:8-1:2 showed a remarkable synergistic effect because during the adsorption process, restacking of the GO nanosheets was inhibited by the CNTs. The theoretical maximum  $\text{Gd}^{3+}$  adsorption capacity of  $534.76 \text{ mg g}^{-1}$  ( $t = 60 \text{ min}$ ,  $\text{pH} = 5.9$ , and  $T = 303 \text{ K}$ ) with an 86.42% increase compared to GO was exhibited by the hybrids having  $M_{\text{CNTs}} : M_{\text{GO}} = 1:6$ . Moreover, a sorption capacity of  $347.83 \text{ mg g}^{-1}$  was retained in the fourth cycle, indicating its exceptional regeneration performance.

Recently, an ultra-lightweight and robust 3D graphene/polydopamine-modified MWCNT hybrid aerogel with

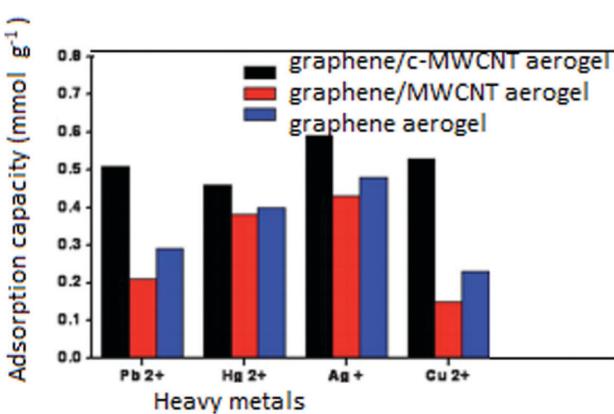
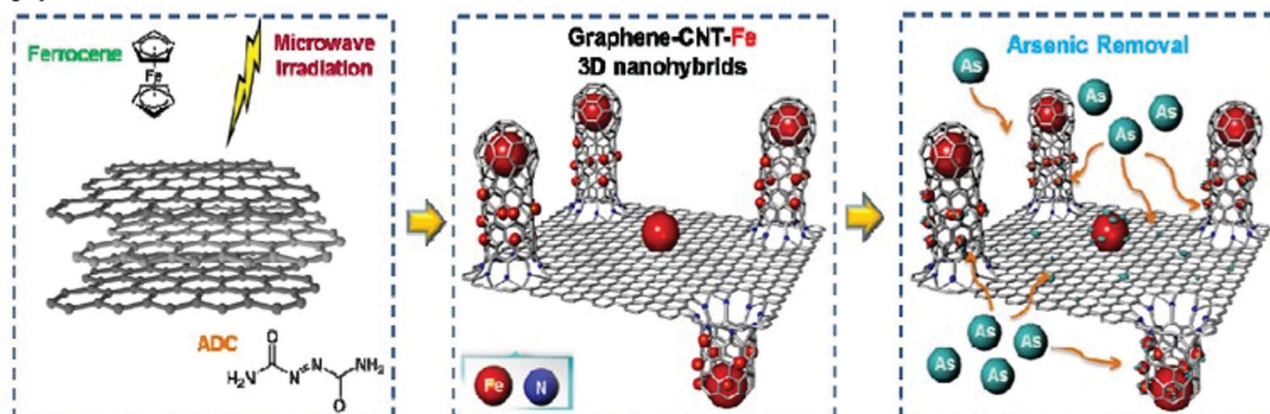


Fig. 7 Adsorption capacity of graphene/MWCNT hybrid aerogels for heavy metal ions. The related adsorption capacity of the graphene alone aerogel is also shown for comparison. Reproduced from ref. 84 with permission from The Royal Society of Chemistry.



## (a) Scheme



## (b) Mechanism

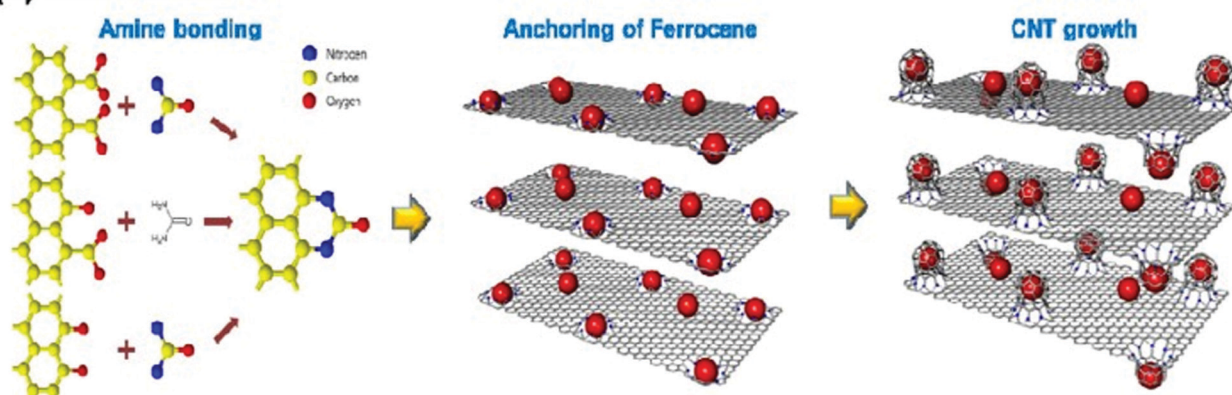


Fig. 8 (a) Growth of CNTs on graphene. (b) Amino functionalization of graphene sheets. Reproduced from ref. 117 with permission from the American Chemical Society.

adsorption capacities as large as  $318.47 \text{ mg g}^{-1}$  for  $\text{Cu}^{2+}$  and  $350.87 \text{ mg g}^{-1}$  for  $\text{Pb}^{2+}$  was synthesised.<sup>122</sup> The synergistic effects of surface complexation and chelation between the

active sites in the hybrid aerogel and metal ions caused the exceptionally high adsorption. In another report, a graphene/CNT hybrid was added to the structure of activated carbon (AC) to improve the adsorption of  $\text{Mn}^{2+}$  from aqueous solutions.<sup>123</sup> The maximum adsorption exhibited for the AC/G/CNT composite of 96.18% was greater than that for AC (89.38%) after 30 min. The introduction of the G/CNT hybrid enhanced the efficiency by 7.5% under same conditions by creating more pores and improving the surface properties of AC.

Graphene/CNT hybrid materials can effectively be employed as an environmentally friendly sensing electrodes for the detection of heavy metal ions, which are much better than either graphene or CNT alone. In this regard, Huang *et al.* prepared 3D graphene/MWCNT hybrid nanocomposites *via* the direct electrochemical reduction of GO-MWCNT nanocomposites. The glassy carbon electrode (GCE) modified with the G-MWCNTs exhibited high sensitivity for the electrochemical detection of trace amounts of  $\text{Cd}^{2+}$  and  $\text{Pb}^{2+}$  ions, with the lowest detection concentration of  $0.5 \mu\text{g L}^{-1}$  for  $\text{Cd}^{2+}$  and  $0.5 \mu\text{g L}^{-1}$  for  $\text{Pb}^{2+}$ . The synergistic effect of MWCNTs and graphene improved the preconcentration efficiency of metal ions and accelerated the electron transfer rate at the G-MWCNT/electrolyte interface, which led to an enhanced detection sensitivity.<sup>124</sup>

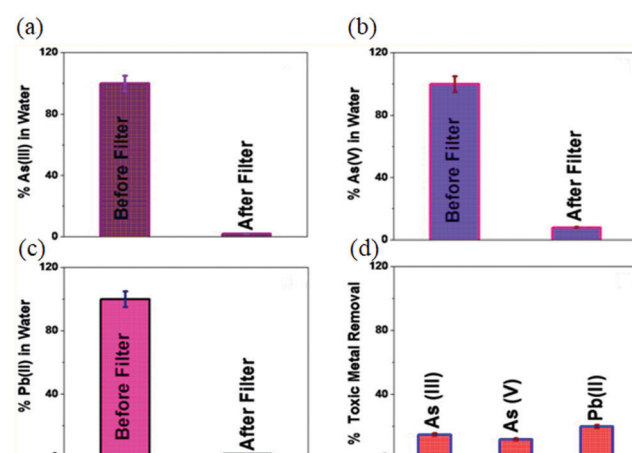


Fig. 9 (a)  $\text{As}^{3+}$ , (b)  $\text{As}^{5+}$ , and (c)  $\text{Pb}^{2+}$  removal efficiency using 3D GO membrane bridged with glutathione-conjugated CNT. (d) Removal efficiency for 3D GO membrane bridged with CNT. Reproduced from ref. 118 with permission from the American Chemical Society.

Hybrid structures of functionalized CNTs and graphene-based materials exhibit outstanding selectivity and high sensitivity for metal ions. In this regard, self-assembled electrochemically cleaved graphene sheets (EGNs) and xanthate-functionalized CNT hybrids were developed to fabricate an improved carbon paste electrode for an electrochemical sensor with high sensitivity and specificity. EGNs improved the electrical conductivity of the hybrid electrode. Additionally, the introduction of EGNs dispersed the functionalized carbon nanotubes to enlarge the electroactive surface area, which possessed a large number of active reaction sites for electrochemical reactions.<sup>125</sup> Owing to their fast electron transfer and much better adsorption, they exhibited good response and specificity for the detection of  $\text{Cu}^{2+}$ .

Double-walled carbon nanotube-graphene hybrid thin films synthesized on copper foil *via* chemical vapour deposition under low pressure exhibited high transparency with 94.3% transmittance. This hybrid material when transferred onto the surface of screen-printed electrodes enhanced the surface area by 1.4 times and electrochemical current by 2.4 times, which was employed for the enzymatic electrochemical detection of  $\text{As}^{5+}$ . The fabricated sensor exhibited good stability, precision and excellent reproducibility.<sup>126</sup>

Recently, a glassy carbon electrode (GCE) modified with an electrochemically reduced GO-MWCNT-L-cysteine (ErGO-MWNTs-L-cys) nanocomposite using the drop-casting method was successfully employed for the detection of lead ions. The presence of rich  $-\text{NH}_2$  groups, large surface area and electrical conductivity of the composite significantly improved the selectivity and sensitivity for the detection of lead ions. The voltammograms of from differential pulse anodic stripping voltammetry illustrated that the anodic peak currents were directly proportional to the concentration of lead ions in the range of 0.2–40  $\mu\text{g L}^{-1}$  with a limit of detection of 0.1  $\mu\text{g L}^{-1}$  ( $\text{S/N} = 3$ ). Moreover, the nanocomposite-modified GCE exhibited satisfactory reproducibility and stability, and hence is suitable for the fabrication of stable sensors.<sup>127</sup> Thus, graphene–CNT hybrid-based sorbents hold great promise for potential applications in the detection and removal of metal ions.

## 5. Gas sensors

The development of gas sensors that can operate at room temperature has attracted considerable attention owing to their excellence in avoiding high temperature, which leads to easy integration, power consumption at a low level and good stability.<sup>128</sup> However, semiconductor metal oxide-based gas sensors demand high temperature for activating their semiconductor properties for the detection of gases, limiting their application for gas sensing at room temperature.<sup>129</sup>

Carbon nanostructures exhibit great potential for gas sensing applications owing to their strong covalent bonds, high stability under diverse environmental conditions, unique electronic properties, low cost and ease of composite formation. Owing to its large surface area and unique electrical

properties, graphene is suitable for efficient gas sensing applications. At room temperature, mechanically exfoliated graphene sheets utilized in gas sensing devices exhibited remarkably low detection noise levels.<sup>130</sup> However, despite the great potential demonstrated by graphene for application in chemical sensors, its mass production and integration into device architecture are challenging for the viable fabrication of sensors. Even though cost-effective methods for the large-scale fabrication of graphene have been achieved *via* chemical exfoliation and used for  $\text{NO}_2$  sensors, its response was unstable and relatively weak.<sup>131,132</sup> CNTs also exhibit outstanding potential for the detection of several gases.<sup>128,133</sup> Even though a more rapid and larger gas sensing response is shown by CNTs than that of graphene, the integration of CNTs onto flexible substrates is a big challenge owing to their imperfect contact with metal electrodes. Moreover, the slow recovery of CNT-based gas sensors and complexity of their fabrication limit their applications. Accordingly, 3D carbon nanostructures made of CNTs and graphene are suitable candidates for the fabrication of gas sensors operating at room temperature owing to their excellent chemical and physical stability, large surface area, high carrier mobility at room temperature and detectable resistance change after adsorption or desorption.

In this regard, a flexible  $\text{NO}_2$  sensor employing hybrid films of vertical CNTs and reduced graphene was developed.<sup>134</sup> The sensor was prepared using a PI substrate (polyimide), gold electrode, hybrid films of CNTs/reduced graphene and an Ni/Cu micro heater. After 60 min exposure, the reduced graphene films exhibited no noticeable  $\text{NO}_2$  sensing, whereas the growth of vertical CNT arrays on the surface of reduced graphene increased the sensitivity by 20%. Moreover, an increase in resistance was observed with a 15 mm bending radius. Stable sensing performances even at extreme bending stress were achieved owing to the exceptional flexibility of reduced graphene.

Kaniyoor and Ramaprabhu synthesised G/MWCNT hybrids *via* the solution phase mixing of graphene suspensions and MWCNT.<sup>135</sup> The aggregation of graphene was further prevented by dispersing nanoparticles of Pt into the hybrids. Using Nafion, the ternary hybrid was solubilized and the drop-casting method was used to fabricate a sensor. At room temperature, the sensor coated on an  $\text{Al}_2\text{O}_3$  substrate exhibited increased sensitivity to  $\text{H}_2$ . The response time and sensitivity almost linearly increased with the  $\text{H}_2$  concentration. Moreover, the ternary hybrid structure exhibited remarkable stability and repeatability.

In another report, a graphene/CNT 3D hybrid was developed *via* two-step CVD under atmospheric pressure.<sup>136</sup> The developed monolithic graphene foam conformally covered with a dense CNT mesh could be efficiently employed as electrochemical electrodes in sensors. Modification using horseradish peroxidase and Nafion enabled the detection of  $\text{H}_2\text{O}_2$  over a wide range (10  $\mu\text{M}$ –1 mM), exhibiting a high sensitivity of 137.9  $\text{mA M}^{-1} \text{cm}^{-2}$  and detection limit as low as  $\sim 1 \mu\text{M}$  with  $\text{S/N} \sim 17.4$ .

Graphene materials based on rGO have attracted great attraction for gas sensing owing to the controllable tuning of



their semiconductor properties using surface modification, bulk quantity production and low cost.<sup>137,138</sup> However, these sensors experience certain inadequacies of long recovery time and low response, limiting their wide applications. Surface modification of rGO using covalent or noncovalent methods enables the fabrication of highly efficient sensing materials by tuning its semiconductor properties. SnO<sub>2</sub> was employed to modify rGO<sup>139–142</sup> for the detection of nitrogen dioxide, hydrogen sulphide and acetone, but the operating temperature was relatively high. SnO<sub>2</sub>–rGO hybrids operating at low temperature have also been developed,<sup>143–145</sup> but the sensing performances (recovery time, response time and sensitivity) of these sensors require further enhancement for practical applications. Thus to satisfy this requirement, MWCNTs were introduced and rGO–MWCNT–SnO<sub>2</sub> was fabricated *via* the hydrothermal method and a room temperature NO<sub>2</sub> sensor was developed, which exhibited good stability, high selectivity, high response, fast response and high recovery rate.<sup>146</sup>

The integration of CNT and graphene, achieved by coupling through poly(ionic liquid) (PIL) as an inter-linker, resulted in active chemical and temperature sensors.<sup>147</sup> For chemical sensing applications, the hybrid composite could function as a chemo resistor for the detection of various volatile organic compounds at room temperature and exhibited a better performance in sensitivity (at ppm level), faster signal response and lower detection limit compared to graphene-only devices. Moreover, a temperature sensor was also fabricated using the hybrid materials, which exhibited a fast response to a small temperature gradient with high stability and sensitivity.

Interestingly, a surface plasmon resonance (SPR)-based fibre optic sensor was developed for methane gas sensing, where four varieties of probes were made up by coating an unclad core of fibre with silver, and then using any of the sensing over-layers of CNT, rGO, G/CNT and G/CNT/PMMA nanocomposite. The interaction of methane molecules with the sensing over-layer changed the dielectric constant of the sensing layer. With an increase in methane concentration, a red shift was observed in the resonance wavelength. The probe coated using the G/CNT/PMMA nanocomposite over-layer showed higher selectivity for methane gas than that with the CNT, rGO, and G/CNT sensing over-layers. Moreover, the doping concentration of 5 wt% G/CNT gave the maximum sensitivity.<sup>148</sup>

Another significant factor affecting the performance of sensing devices is humidity. A hydrophobic sensing material operating at room temperature was developed by depositing hybrid films of MWCNT/graphene on an Ni substrate employing microwave plasma-enhanced chemical vapour deposition in the temperature range of 500–700 °C and pressure of 20 torr.<sup>149</sup> For ammonia sensing, a quick response and recovery time of 96 s were observed for the film deposited at 700 °C. Additionally, the hydrophobic surface of the film enabled gas sensing even in a humid environment.

A flexible NO<sub>2</sub> sensor fabricated from a tungsten trioxide nanoparticle-loaded MWCNT/RGO hybrid on a polyimide substrate exhibited a maximum response of 17% to 5 ppm, a short response/recovery time of 7/15 min and low limit of

detection of 1 ppm.<sup>150</sup> Moreover, outstanding mechanical flexibility was observed, even at a bending angle of 90° and after 10<sup>6</sup> cycles of bending/relaxing process.

A 3D hybrid structure of MnO<sub>2</sub>/graphene/CNTs decorated with gold nanoparticles (AuNPs/MnO<sub>2</sub>/G/CNTs), which was sensitive to H<sub>2</sub>O<sub>2</sub>, was developed *via* a three-step method.<sup>151</sup> The MnO<sub>2</sub> nanoparticles attached to the G/CNT network served as the active element for sensing H<sub>2</sub>O<sub>2</sub>. The uniformly distributed gold nanoparticles on the surface of the MnO<sub>2</sub> particles provided further active sites for adsorbing H<sub>2</sub>O<sub>2</sub> molecules and enhanced the electrical conductivity of the hybrid. The AuNP/MnO<sub>2</sub>/G/CNT hybrids exhibited outstanding electrocatalytic activity for H<sub>2</sub>O<sub>2</sub> with appreciable sensitivity of 452 μA mM<sup>−1</sup> cm<sup>−2</sup> and low detection limit of 0.1 μM (S/N = 3).

3D graphene–CNT structures synthesized by CVD were decorated with TiO<sub>2</sub> nanoparticles *via* the sparking method and efficiently utilized for toluene sensing at room temperature. The response for toluene was enhanced by more than 7 times upon decoration using TiO<sub>2</sub> nanoparticles. 3D TiO<sub>2</sub>/G-CNT had shown significantly greater selectivity and sensitivity than graphene, CNTs, 3D G-CNT and TiO<sub>2</sub>–CNT over a concentration range of 50–500 ppm at room temperature.<sup>152</sup>

An ammonia sensor employing Sn–TiO<sub>2</sub>/rGO/CNT nanocomposites was fabricated by Seekaew, Pon-On *et al.*, which exhibited outstanding response together with superior selectivity to ammonia among various environmental gases and volatile organic compounds at room temperature.<sup>153</sup> The gas sensor having a molar ratio of Sn/Ti = 1:10 exhibited the maximum response to NH<sub>3</sub> among the ratios and pure Sn–TiO<sub>2</sub> and rGO/CNT gas sensors.

A flexible and fully transparent UV sensor made up of photoactive CNT networks and graphene electrodes was reported with an improved photoresponse (30 times higher) in comparison to a CNT–Au sensor.<sup>154</sup> The similar molecular structure of CNT and graphene resulted in low contact resistance between them, and hence enabled efficient charge transfer (Fig. 10). Moreover, the CNT/graphene UV sensor exhibited over 80% optical transparency at 550 nm and exceptional mechanical flexibility without substantial variation in electrical resistance over 500 cycles against external bending.

Recently, an optoelectronic device for NO<sub>2</sub> sensing at room temperature was developed using an MoS<sub>2</sub>/rGO hybrid on vertically aligned CNTs.<sup>155</sup> Together with an ohmic contact with the hybrid material, the vertically aligned CNT produced a weak charge impurity scattering in the rGO layers, which improved the response time by 40% and photo responsivity by 236% compared to that of the gold-contacted device. Moreover, under laser illumination, the complete recovery time of ~150 s and outstanding sensitivity of ~41% at 100 ppm NO<sub>2</sub> were demonstrated, which showed enhancements compared to sensing in the dark.

The adsorption of gases by 3D graphene/CNT networks is a relatively unexplored field of study, with only a few articles published in the past few years reporting graphene foams as adsorbents of CO<sub>2</sub>,<sup>156,157</sup> acetone<sup>158</sup> and formaldehyde.<sup>159</sup> However, MWCNTs and graphene oxide were individually used



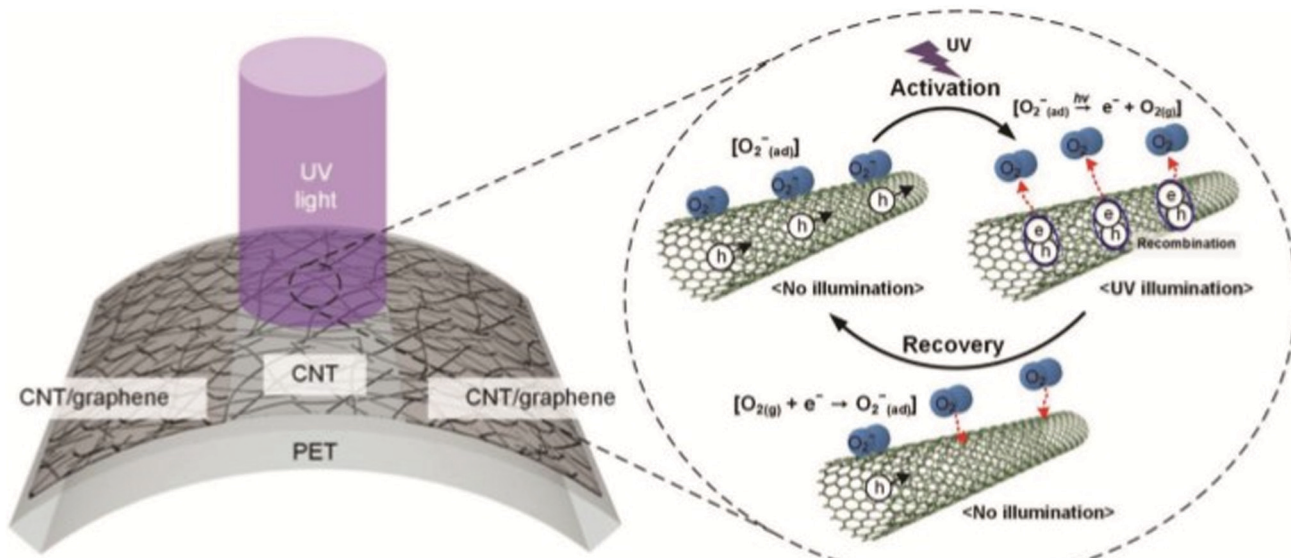


Fig. 10 CNT/graphene UV sensor. Photo detection mechanism: CNT networks connect the graphene electrodes. In ambient air, CNT is p-doped by  $O_2^-$  adsorbed on its surface. UV light illumination causes oxygen desorption, and hence reduction in hole concentration in CNT, which leads to an increase in electrical resistance. Reproduced from ref. 154 with permission from John Wiley and Sons.

as efficient supports for layered double hydroxides (LDH) for enhancing the  $CO_2$  sorption capacity of adsorbents, but their stability subjected to TSA (temperature-swing adsorption) cycles required improvement. To satisfy this, GO/MWCNT hybrid systems were prepared with an enhanced surface area, greater stability and compatibility for the active LDH material.<sup>160</sup> The incorporated hybrid carbon network enhanced the thermal stability of LDH for over 20 cycles and intensely reduced the sintering observed with either MWCNT or GO separately. Moreover, equal proportions of MWCNT and GO resulted in maximum sorption (Fig. 11).

An interesting aerogel of carbon nanotube-enhanced amino-functional graphene was synthesised by adding CNTs into graphene oxide solution and reducing them using ethylene diamine.<sup>161</sup> The improved microstructure of the aerogel and  $-NH_2$  groups on the graphene layer improved the chemical and physical adsorption of formaldehyde. The breakthrough time of the aerogel of  $20\,300\,min\,g^{-1}$  was greater than that of reduced graphene aerogels. Moreover, the aerogel exhibited an adsorption capacity of  $27.43\,mg\,g^{-1}$ . The results showed that together with physical adsorption, chemical adsorption also

enhanced the removal of formaldehyde. Thus, in the future, the integration of graphene–CNT hybrids in sensing devices can enable effective environmental monitoring and remediation.

## 6. Catalytic conversion of pollutants

For the removal of toxic chemicals, various methods such as adsorption, catalytic reduction and photocatalytic degradation have been used.<sup>162,163</sup> To achieve efficient pollutant transformation, high adsorption capacity is inevitable. Upon irradiation of a photocatalyst with visible and/or UV light, their valence band electrons get promoted to the conduction band, thereby generating holes. The as-formed electron–hole pairs move to the surface and initiate redox reactions with the adsorbate. However, the catalytic efficiency of semiconductors is largely limited because of their rapid electron–hole pair recombination. In this regard, 3D graphene/CNT hybrids can be employed as a competent platform for the conversion of various contaminants with metal/metal oxide nanoparticles owing to the following reasons. (i) The 3D network structure can adsorb a large quantity of contaminants, (ii) the hybrid structure can function as a suitable framework for the efficient dispersal of the catalyst, which would otherwise aggregate because of its high surface energy and (iii) the well interconnected 3D network facilitates fast charge transportation, preventing electron–hole recombination. Thus, 3D CNT/graphene hybrids exhibit significant potential for the efficient conversion of pollutants.<sup>13</sup>

Graphene-based materials having good electrical conductivity and large surface area were prepared by pillarising GO and rGO with CNTs *via* the chemical vapour deposition method, employing acetonitrile as the carbon source and nickel nanoparticles as the

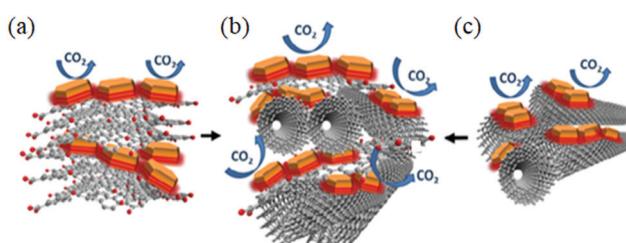


Fig. 11 (a) GO-LDH. (b) Hybrid GO/MWNT-LDH. (c) MWNT-LDH. Reproduced from ref. 160 with permission from Elsevier.



catalyst.<sup>164</sup> The composite material exhibited outstanding performance under visible light-activated photocatalysis for the degradation of Rhodamine B dye owing to its unique porous structure and the excellent electron transfer property of graphene.

For the degradation of methyl orange in the presence of  $\text{H}_2\text{O}_2$  under visible light, 3D CNT/rGO was implanted on  $\text{Cu}_2\text{O}$  composite spheres.<sup>165</sup> The observed degradation on CNTs/rGO/ $\text{Cu}_2\text{O}$  of ~99.8% was much greater than that on rGO/ $\text{Cu}_2\text{O}$  of ~77.6%, CNTs/ $\text{Cu}_2\text{O}$  of ~72.3% and pure  $\text{Cu}_2\text{O}$  spheres of ~67.9%. Under visible illumination, the electrons in the valence band of  $\text{Cu}_2\text{O}$  were excited to the conduction band and transferred to CNTs/rGO, which could collect and transport electrons, leading to electron–hole separation. Meanwhile, the  $\text{H}_2\text{O}_2$  molecules were reduced and the generated  $\cdot\text{OH}$  radicals directly decomposed the dye.

Wang *et al.* synthesised a graphene/MWCNT/TiO<sub>2</sub> hybrid *via* the solvothermal method, which demonstrated improved photocatalytic efficiency over graphene/TiO<sub>2</sub> in the degradation of methylene blue and the reduction of Cr<sup>6+</sup> under UV irradiation.<sup>166</sup> The photocatalytic activity was dependent on the percentage of CNTs in the hybrid and optimal mass ratio observed was MWCNTs: TiO<sub>2</sub> = 5%. CNTs served as charge transmitting paths, thereby decreasing the recombination rate of electron–hole pairs. For the degradation of methylene blue, the apparent rate constant was 2.2 times greater and for the reduction of Cr<sup>6+</sup>, the value was 1.9 times greater than that of the graphene/TiO<sub>2</sub> composite (Fig. 12).

Although adsorption has attracted great attention for the removal of dyes because of its simple design, high efficiency and economic feasibility, it causes second pollution in the course of the recovery of the dyes.<sup>167</sup> In this regard, the catalytic

oxidation of dyes has gained remarkable interest for treating a huge amount of contaminated water with low energy consumption. Especially, catalytic wet peroxide oxidation is effective for removing various organic pollutants on a large scale.<sup>168–170</sup> A ternary hybrid of MnO<sub>2</sub>@CNT-reduced graphene oxide was prepared, which exhibited superior catalytic activity in comparison to MnO<sub>2</sub>@CNT in removing Basic Red 18 dye in the presence of  $\text{H}_2\text{O}_2$  within a short time.<sup>171</sup> Moreover, the hybrid exhibited excellent decolourisation through three successive catalytic wet peroxide oxidations within 30 min.

Although Fe<sub>3</sub>O<sub>4</sub> nanoparticles possess peroxidase-like catalytic activities and high electrocatalytic activity when loaded on CNT supports, their catalytic efficiencies in aqueous systems encounter some challenges owing to the poor dispersion of the hydrophobic CNTs and low stability of the catalysts. In this regard, amphiphilic GO nanosheets were employed to disperse CNTs and a stable G/CNT/Fe<sub>3</sub>O<sub>4</sub> nanocomposite with improved catalytic activity was synthesised.<sup>172</sup> The nanocomposite exhibited more efficient peroxidase-like catalytic activities and electrocatalysis to  $\text{H}_2\text{O}_2$  and superior aqueous stability compared to Fe<sub>3</sub>O<sub>4</sub> nanoparticles and CNT/Fe<sub>3</sub>O<sub>4</sub>. Moreover, the nanocomposite had advantages such as environmental stability, magnetic separation and recyclability.

Interestingly, a composite aerogel of graphene oxide and CNTs decorated with FeOOH nanoparticles was synthesized, which exhibited remarkable catalytic activity for the degradation of methylene blue, Rhodamine B, Orange II, phenol and BPA.<sup>173</sup> The 3D porous network enabled effective charge/mass transfer, thereby improving the catalytic performance of FeOOH. The efficient conversion between Fe<sup>2+</sup>/Fe<sup>3+</sup> and synergistic coupling of FeOOH with the GO/CNT aerogel enhanced the photocatalytic activity of the hybrid.

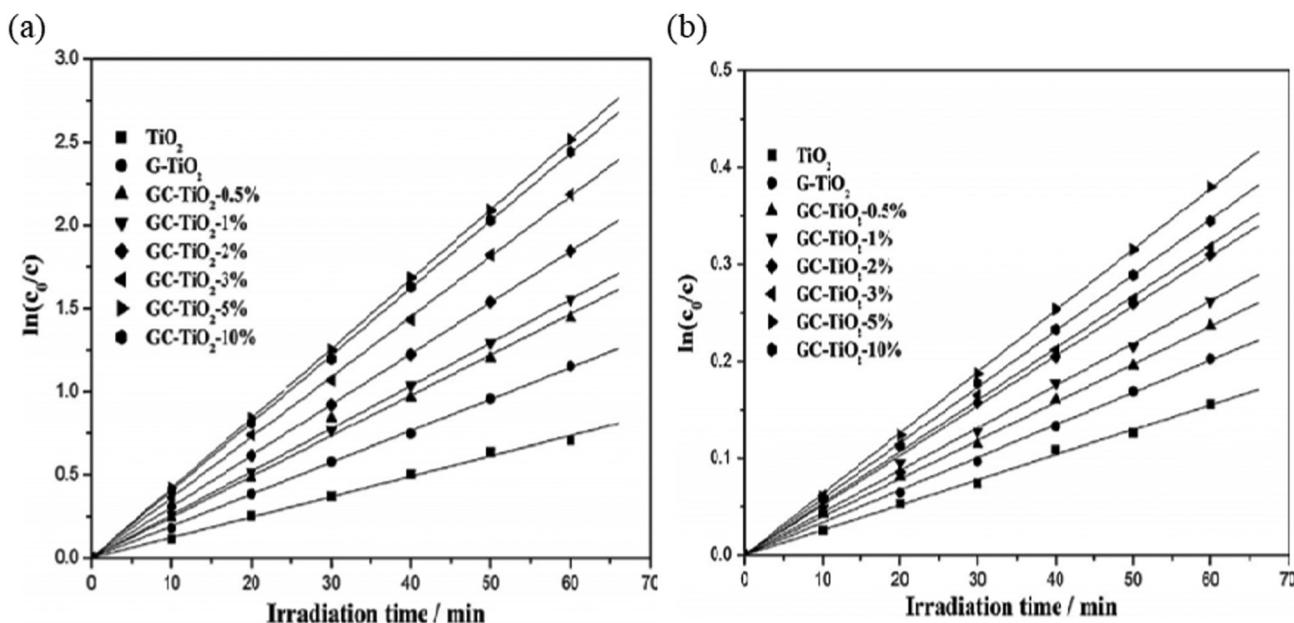


Fig. 12 Linear transformed  $\ln(c_0/c) = kt$  of the kinetic curves of (a) methylene blue degradation and (b) photoreduction of Cr<sup>6+</sup> for TiO<sub>2</sub>, graphene/TiO<sub>2</sub> and graphene/CNT/TiO<sub>2</sub> composites. Reproduced from ref. 166 with permission from Elsevier.



Qu *et al.* prepared a heterostructured nanocomposite by combining oxygen-modified monolayer graphite-like  $C_3N_4$  with GO and nitrogen-doped CNTs, exhibiting outstanding activity for the degradation of Rhodamine 6G in comparison to pure  $O-g-C_3N_4$  and  $O-g-C_3N_4/GO$  under visible light irradiation.<sup>174</sup> GO and nitrogen-doped CNT acted as electronic acceptors and inhibited the recombination of electron-hole pairs (Fig. 13). The nanocomposite was further employed for the removal and degradation of tetracycline hydrochloride in water, which confirmed its catalytic activity and recyclable stability.

In another study, Yi *et al.* reported the synthesis of 3D graphene/CNT-supported copper nanocubes with platinum skin *via* simple electrodeposition and galvanic replacement.<sup>175</sup> The hybrid having a 3D interconnected network enabled quick mass diffusion and rapid electron transfer. Consequently, the hybrid exhibited outstanding electrocatalytic activity and superior durability compared to the Pt/C catalyst towards the methanol oxidation reaction.

Catalytic reduction has gained widespread attention for the removal of toxic chemicals on account of its efficiency, cost effectiveness, simple preparation and energy saving.<sup>176,177</sup> 3D N-doped graphene–CNT networks well encapsulated with Ni nanoparticles were synthesised using Ni-based MOFs (metal organic frameworks) and melamine as precursors.<sup>178</sup> Among the various products obtained, that pyrolyzed at 800 °C exhibited an outstanding performance of ~99.6% reduction of  $Cr^{6+}$  with HCOOH, owing to the synergistic effects of the porous 3D network together with high N-doping level and enormous ultrafine Ni nanoparticles (Fig. 14). In addition, its microstructure and catalytic efficiency remained unchanged even after the 10th recycling, signifying its exceptional stability.

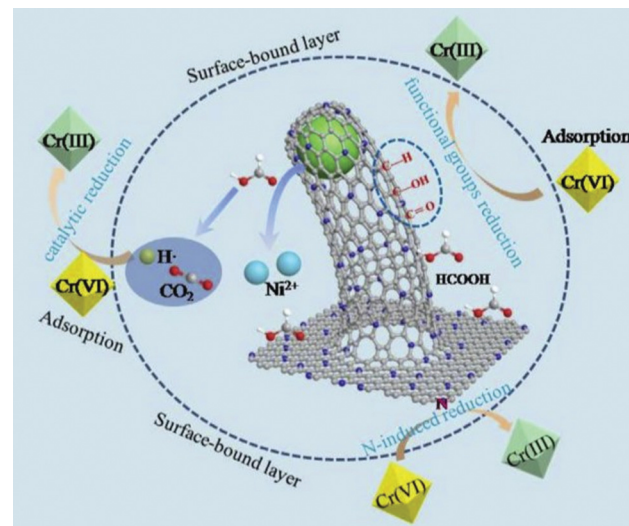


Fig. 14  $Cr^{6+}$  reduction with HCOOH using 3D Ni@N-CNTs/N-G. Reproduced from ref. 178 with permission from Elsevier.

Tran *et al.* reported the eco-friendly and simple synthesis of a partially reduced GO/CNT/Fe/Ag hybrid within 10–30 s *via* simple microwave irradiation.<sup>179</sup> During the reduction of 4-nitrophenol using NaBH<sub>4</sub>, the hybrid exhibited exceptional catalytic efficiency with a rate constant of ~ $14.66 \times 10^{-3} \text{ s}^{-1}$ . By utilizing its large surface area, graphene oxide helped to immobilize more Ag nanoparticles and rGO/CNT promoted electron transfer in the reduction of 4-nitrophenol owing to its high electrical conductivity. Fe nanoparticles and Fe<sub>3</sub>C enabled easy recovery with the help of an external magnet. Moreover, the hybrid retained stability and catalytic efficiency even after the 5th cycle.

In another interesting study, sorption and catalysis were simultaneously realized for the effective removal of  $As^{5+}$  and  $Se^{6+}$  over magnetic GO/oxidized CNT hydrogels.<sup>180</sup> Sorption facilitated the catalytic reactions; meanwhile, catalytic reduction supported the release of the occupied sorption sites, and thus resumed another sorption-catalysis cycle. The insertion of oxidized CNTs increased the pore volume and specific surface area of the GO hydrogel, which enabled a further enhanced decontamination performance. The hybrid exhibited an outstanding decontamination capacity of  $258.2 \text{ mg g}^{-1}$  for  $As^{5+}$  and  $46.2 \text{ mg g}^{-1}$  for  $Se^{6+}$ . Ultra-fast removal equilibriums were identified within 9 min for  $As^{5+}$  and 2 min for  $Se^{6+}$ ; moreover, remarkable stability was also exhibited in repeated experiments.

Organic pollutants were removed efficiently by employing magnetic CNT/rGO decorated with silver nanoparticles.<sup>181</sup> For generating magnetic carbon nanotubes, Fe<sub>3</sub>O<sub>4</sub> nanoparticles were grown and anchored on MWCNT, and then coated with polydopamine to introduce new surface functionalities. Hydrothermal treatment with GO resulted in reduced GO/polydopamine/magnetic CNT, which exhibited outstanding adsorption capability. The deposition of silver nanoparticles on the nanocomposite integrated an efficient catalytic performance in the removal of methylene blue and 4-nitrophenol.

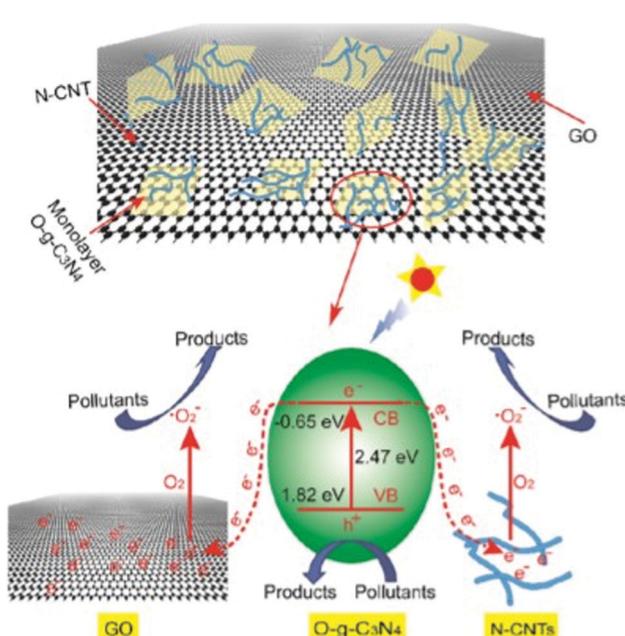


Fig. 13 Electron transfer and photocatalytic degradation of pollutants by  $O-g-C_3N_4/GO/N-CNT$  under visible light irradiation. Reproduced from ref. 174 with permission from the American Chemical Society.



Moreover, easy regeneration of the nanocomposite *via* desorption using ethanol and water (for more than 15 cycles) and easy magnetic separation show great potential in wastewater treatment.

Kotal and coworkers developed a graphene-assisted Co nanoparticle-embedded nitrogen-doped CNT (G/Co/NCNT) hybrid *via* the controlled annealing of GO-ZIF-67 under an Ar atmosphere for the photocatalytic degradation of Reactive Black 5 under visible light.<sup>182</sup> The high surface area of graphene enabled greater ZIF-67 decoration, thereby the growth of NCNTs was higher in the G/Co/NCNT hybrid compared to Co/NCNT. A higher amount of nitrogen doping led to lowering of the band gap and enhanced photocatalytic activity. The hybrid demonstrated 98% degradation ability after 60 min, had wide pH tolerance and recyclability even after 5 cycles under visible light.

## 7. Environmental impacts of graphene/carbon nanotube hybrids

The environmental impact of nanomaterials is a matter of concern nowadays, which should be evaluated critically. Understanding the total impact of a process or product on the environment is an inevitable part of green manufacturing and a green product. Evaluation of the total life cycle of a product from raw materials, manufacturing, use, and ultimate reuse/disposal should be performed seriously to maintain environmental sustainability. Life cycle analysis (LCA) is a systematic tool that can be used to study and analyse strategies to meet environmental challenges. The life-cycle paradigm necessitates the consideration of not only the immediate impacts of a process or product, but also its long-term response.<sup>183</sup> The outcome of LCA can have a positive impact on the ecosystem, human health and natural resources.

Both graphene and carbon nanotubes are resistant to harsh environments. Moreover, they offer good recycling capabilities. The regeneration of graphene and CNT has been studied using acids and bases, making the recovery of contaminants feasible. In certain cases, batch methods appear to be more efficient for contaminant adsorption than fixed bed methods. This choice will allow the maximum adsorption with to be obtained with the minimum amount of adsorbent, thereby reducing the quantities of harmful waste to be treated.<sup>184</sup> Both graphene and CNT have been investigated to evaluate their environmental impact and toxicity. Studies on zebra fish have revealed that their cardiac rates and growth are affected by exposure to carbon nanotubes.<sup>185</sup> It has also been reported that CNT can interact with biomolecules in water and cause toxic effects.<sup>186</sup>

Even though graphene is considered a chemically stable material, changes in pH affect the protonation of its hydroxyl or carbonyl groups. At low pH, graphene tends to form aggregates, at high pH it dissolves like a salt, while at neutral pH it stays suspended in the solution.<sup>187</sup> The stability of graphene oxide depends on its particle size and functional groups on its surface.<sup>188</sup> In this scenario, its dose-related toxicity can vary.

Overall, the formation of colloids should be absolutely avoided. Owing to the hydrophilic nature of graphene oxide nanosheets, they can be dispersed in aqueous solution, thereby demonstrating different dispersion performances in comparison to pristine graphene and reduced graphene.<sup>189</sup> Therefore, insight into the variability of graphene is essential to understand the interaction, adsorption, transformation, and toxicity criteria of graphene. However, the effect of graphene on the human body is still unknown, although graphene oxide is known to accumulate in the lungs of mice when inhaled, but no pathological outcome was further reported.

To the best of our knowledge, there is very little information available on the risks of exposure to graphene/CNT hybrid materials for both humans and animals and their long-lasting environmental problems. Thus, to efficiently utilize these materials in environmental remediation systems, their release and disposal need to be properly planned and evaluated. Life cycle analysis of these hybrid materials is a potential research area that has to be explored.

## 8. Conclusion and future perspectives

Environmental pollution by water-soluble pollutants, heavy metal ions and harmful greenhouse gases is triggering significant concern worldwide. Immense progress had already achieved in the synthesis, composite formation and potential applications of graphene/CNT hybrid materials for environmental monitoring, sensing and remediation. The adsorption of various pollutants such as oils, organic solvents and dyes by these hybrid materials is appreciable owing to their facile synthetic methods, high adsorption capability, stable cyclic performance, low cost, easy operation, simple processes and little damage to the environment. Moreover, by employing electrostatic interactions, ion exchange process and surface complexation with metal ions, these materials are widely used for removing metals owing to their high efficiency, simple design, ease of operation, low maintenance cost and capability of metal recovery. Furthermore, with their tuneable pore size and huge surface area, these materials are very effective for the capture of gaseous pollutants.

Although great progress has been attained in this field, further research in real-life situations is necessary. To promote further research and practical applications, the following challenges need to be the focus. (i) Considering that various adsorption mechanisms simultaneously occur on the surface of GO and CNTs, which vary with changes in surface functionalization and environmental test conditions, more studies regarding these mechanisms are necessary. (ii) Further research to control the functional groups on the surface of graphene to couple selective adsorption characteristics and ultimate hydrophobicity is essential in this area. (iii) Even though these hybrid materials can provide uniform 3D nanofiltration membranes, which result in elevated permeability and separation capability, studies regarding their practical separation applications are limited. (iv) Although graphene/CNT hybrid materials can be effectively employed as environment-friendly sensing electrodes for the detection of heavy



metal ions, studies regarding this are limited. (v) Similarly, these 3D hybrid materials have been found to be effective in gas sensing; however, studies on the capture of gaseous pollutants are in their initial stage. Whether they are capable of carbon capture and even take-over of dust in the atmosphere or indoor environment needs to be examined. (vi) The catalytic conversion of pollutants using these hybrid materials requires further investigation relating to some critical issues regarding their activity and stability enhancement mechanisms. Moreover, many techniques presented in this review are on the laboratory level, their commercialization requires further research.

There are numerous environmental pollutants, only a few of which have been explored to date. Thus, further research to develop smart porous membranes and exploitation of the immense sensing applications of these materials to develop efficient sensing devices is anticipated in the near future. Moreover, for the efficient utilization of these materials in environmental remediation systems, their life cycle analysis is inevitable. This is a potential research area to be explored. It is anticipated that the boundless scope of these 3D hybrid materials will enable the control of environmental pollution, resulting in a sustainable world.

## Author contributions

Jomol P. John: conceptualization, resources, writing, reviewing and editing. Mary Nancy T. E.: conceptualization, resources. Bindu Sharmila T. K.: conceptualization, supervision, reviewing and editing.

## Conflicts of interest

There are no conflicts of interest to declare.

## References

- 1 A. K. Geim and K. S. Novoselov, The rise of graphene, *Nat. Mater.*, 2007, **6**(3), 183–191.
- 2 C. Rao, H. R. Matte and K. Subrahmanyam, Synthesis and selected properties of graphene and graphene mimics, *Acc. Chem. Res.*, 2013, **46**(1), 149–159.
- 3 Y. Zhu, H. Ji, H.-M. Cheng and R. S. Ruoff, Mass production and industrial applications of graphene materials, *Natl. Sci. Rev.*, 2018, **5**(1), 90–101.
- 4 K. S. Novoselov, D. Jiang, F. Schedin, T. Booth, V. Khotkevich and S. Morozov, *et al.*, Two-dimensional atomic crystals, *Proc. Natl. Acad. Sci. U. S. A.*, 2005, **102**(30), 10451–10453.
- 5 N. Behabtu, J. R. Lomeda, M. J. Green, A. L. Higginbotham, A. Sinitskii and D. V. Kosynkin, *et al.*, Spontaneous high-concentration dispersions and liquid crystals of graphene, *Nat. Nanotechnol.*, 2010, **5**(6), 406–411.
- 6 Y. Zhu, L. Li, C. Zhang, G. Casillas, Z. Sun and Z. Yan, *et al.*, A seamless three-dimensional carbon nanotube graphene hybrid material, *Nat. Commun.*, 2012, **3**(1), 1–7.
- 7 G. K. Dimitrakakis, E. Tylianakis and G. E. Froudakis, Pillared graphene: a new 3-D network nanostructure for enhanced hydrogen storage, *Nano Lett.*, 2008, **8**(10), 3166–3170.
- 8 D. Kondo, S. Sato and Y. Awano, Self-organization of novel carbon composite structure: graphene multi-layers combined perpendicularly with aligned carbon nanotubes, *Appl. Phys. Express*, 2008, **1**(7), 074003.
- 9 S. Azizighannad and S. Mitra, Controlled synthesis of reduced graphene oxide–carbon nanotube hybrids and their aqueous behavior, *J. Nanoparticle Res.*, 2020, **22**(6), 130.
- 10 V. T. Dang, D. D. Nguyen, T. T. Cao, P. H. Le, D. L. Tran and N. M. Phan, *et al.*, Recent trends in preparation and application of carbon nanotube–graphene hybrid thin films, *Adv. Natl. Sci.: Nanosci. Nanotechnol.*, 2016, **7**(3), 033002.
- 11 S. Nardeccchia, D. Carriazo, M. L. Ferrer, M. C. Gutiérrez and F. del Monte, Three dimensional macroporous architectures and aerogels built of carbon nanotubes and/or graphene: synthesis and applications, *Chem. Soc. Rev.*, 2013, **42**(2), 794–830.
- 12 X. Wu, F. Mu and H. Zhao, Recent progress in the synthesis of graphene/CNT composites and the energy-related applications, *J. Mater. Sci. Technol.*, 2020, **55**, 16–34.
- 13 A. Dasgupta, L. P. Rajukumar, C. Rotella, Y. Lei and M. Terrones, Covalent three-dimensional networks of graphene and carbon nanotubes: synthesis and environmental applications, *Nano Today*, 2017, **12**, 116–135.
- 14 X. Dong, J. Chen, Y. Ma, J. Wang, M. B. Chan-Park and X. Liu, *et al.*, Superhydrophobic and superoleophilic hybrid foam of graphene and carbon nanotube for selective removal of oils or organic solvents from the surface of water, *Chem. Commun.*, 2012, **48**(86), 10660–10662.
- 15 B. Yu, J. Xu, J.-H. Liu, S.-T. Yang, J. Luo and Q. Zhou, *et al.*, Adsorption behavior of copper ions on graphene oxide–chitosan aerogel, *J. Environ. Chem. Eng.*, 2013, **1**(4), 1044–1050.
- 16 Z.-Y. Wu, C. Li, H.-W. Liang, Y.-N. Zhang, X. Wang and J.-F. Chen, *et al.*, Carbon nanofiber aerogels for emergent cleanup of oil spillage and chemical leakage under harsh conditions, *Sci. Rep.*, 2015, **4**(1), 4079.
- 17 M. S. Mauter and M. Elimelech, Environmental Applications of Carbon-Based Nanomaterials, *Environ. Sci. Technol.*, 2008, **42**(16), 5843–5859.
- 18 X. Dong, G. Xing, M. B. Chan-Park, W. Shi, N. Xiao and J. Wang, *et al.*, The formation of a carbon nanotube–graphene oxide core–shell structure and its possible applications, *Carbon*, 2011, **49**(15), 5071–5078.
- 19 A. L. Gorkina, A. P. Tsapenko, E. P. Gilshteyn, T. S. Koltsova, T. V. Larionova and A. Talyzin, *et al.*, Transparent and conductive hybrid graphene/carbon nanotube films, *Carbon*, 2016, **100**, 501–507.
- 20 C. Zhang, L. Ren, X. Wang and T. Liu, Graphene Oxide-Assisted Dispersion of Pristine Multiwalled Carbon Nanotubes in Aqueous Media, *J. Phys. Chem. C*, 2010, **114**(26), 11435–11440.



21 L. L. Zhang, Z. Xiong and X. Zhao, Pillaring chemically exfoliated graphene oxide with carbon nanotubes for photocatalytic degradation of dyes under visible light irradiation, *ACS Nano*, 2010, **4**(11), 7030–7036.

22 S. Badhulika, T. Terse-Thakoor, C. M. Chaves Villarreal and A. Mulchandani, Graphene hybrids: synthesis strategies and applications in sensors and sensitized solar cells, *Front. Chem.*, 2015, **3**, 38.

23 W. Fan, L. Zhang and T. Liu, Strategies for the Hybridization of CNTs with Graphene in *Graphene-Carbon Nanotube Hybrids for Energy and Environmental Applications*, Springer, 2017, pp. 21–51.

24 D. V. Kosynkin, A. L. Higginbotham, A. Sinitskii, J. R. Lomeda, A. Dimiev and B. K. Price, *et al.*, Longitudinal unzipping of carbon nanotubes to form graphene nanoribbons, *Nature*, 2009, **458**(7240), 872–876.

25 R. Paul, M. Vincent, V. Etacheri and A. K. Roy, Carbon nanotubes, graphene, porous carbon, and hybrid carbon-based materials: synthesis, properties, and functionalization for efficient energy storage in *Carbon Based Nanomaterials for Advanced Thermal and Electrochemical Energy Storage and Conversion*, Elsevier, 2019, pp. 1–24.

26 S. S. J. Aravind, V. Eswaraiah and S. Ramaprabhu, Facile synthesis of one dimensional graphene wrapped carbon nanotube composites by chemical vapour deposition, *J. Mater. Chem.*, 2011, **21**(39), 15179–15182.

27 Y. Li, Z. Li, L. Lei, T. Lan, Y. Li and P. Li, *et al.*, Chemical vapor deposition-grown carbon nanotubes/graphene hybrids for electrochemical energy storage and conversion, *FlatChem*, 2019, **15**, 100091.

28 A. Kumar, K. Sharma and A. R. Dixit, Carbon nanotube- and graphene-reinforced multiphase polymeric composites: review on their properties and applications, *J. Mater. Sci.*, 2020, **55**(7), 2682–2724.

29 Y. Shen, Q. Fang and B. Chen, Environmental Applications of Three-Dimensional Graphene-Based Macrostructures: Adsorption, Transformation, and Detection, *Environ. Sci. Technol.*, 2015, **49**(1), 67–84.

30 Y. Cheng, P. Xu, W. Zeng, C. Ling, S. Zhao and K. Liao, *et al.*, Highly hydrophobic and ultralight graphene aerogel as high efficiency oil absorbent material, *J. Environ. Chem. Eng.*, 2017, **5**(2), 1957–1963.

31 S. Kizil, Bulbul Sonmez H. One-pot fabrication of reusable hybrid sorbents for quick removal of oils from wastewater, *J. Environ. Manage.*, 2020, **261**, 109911.

32 R.-P. Ren, W. Li and Y.-K. Lv, A robust, superhydrophobic graphene aerogel as a recyclable sorbent for oils and organic solvents at various temperatures, *J. Colloid Interface Sci.*, 2017, **500**, 63–68.

33 V. K. Sharma, T. J. McDonald, H. Kim and V. K. Garg, Magnetic graphene–carbon nanotube iron nanocomposites as adsorbents and antibacterial agents for water purification, *Adv. Colloid Interface Sci.*, 2015, **225**, 229–240.

34 S. Hou, X. Wu, Y. Lv, W. Jia, J. Guo and L. Wang, *et al.*, Ultralight, highly elastic and bioinspired capillary-driven graphene aerogels for highly efficient organic pollutants absorption, *Appl. Surf. Sci.*, 2020, **509**, 144818.

35 J. Huang and Z. Yan, Adsorption mechanism of oil by resilient graphene aerogels from oil–water emulsion, *Langmuir*, 2018, **34**(5), 1890–1898.

36 H. Wang, C. Wang, S. Liu, L. Chen and S. Yang, Superhydrophobic and superoleophilic graphene aerogel for adsorption of oil pollutants from water, *RSC Adv.*, 2019, **9**(15), 8569–8574.

37 W. Wan, F. Zhang, S. Yu, R. Zhang and Y. Zhou, Hydrothermal formation of graphene aerogel for oil sorption: the role of reducing agent, reaction time and temperature, *New J. Chem.*, 2016, **40**(4), 3040–3046.

38 M. Inagaki, A. Kawahara and H. Konno, Sorption and recovery of heavy oils using carbonized fir fibers and recycling, *Carbon*, 2002, **40**(1), 105–111.

39 A. M. Atta, R. A. M. El-Ghazawy, R. K. Farag and A. A. A. Abdel-Azim, Swelling and Network Parameters of Oil Sorbers Based on Alkyl Acrylates and Cinnamoyloxy Ethyl Methacrylate Copolymers, *J. Polym. Res.*, 2006, **13**(4), 257–266.

40 V. Janout, S. B. Myers, R. A. Register and S. L. Regen, Self-Cleaning Resins, *J. Am. Chem. Soc.*, 2007, **129**(17), 5756–5759.

41 T. Ono, T. Sugimoto, S. Shinkai and K. Sada, Lipophilic polyelectrolyte gels as super-absorbent polymers for non-polar organic solvents, *Nat. Mater.*, 2007, **6**(6), 429–433.

42 T. Ono, T. Sugimoto, S. Shinkai and K. Sada, Molecular Design of Superabsorbent Polymers for Organic Solvents by Crosslinked Lipophilic Polyelectrolytes, *Adv. Funct. Mater.*, 2008, **18**(24), 3936–3940.

43 J. Yuan, X. Liu, O. Akbulut, J. Hu, S. L. Suib and J. Kong, *et al.*, Superwetting nanowire membranes for selective absorption, *Nat. Nanotechnol.*, 2008, **3**(6), 332–336.

44 A. Sayari, S. Hamoudi and Y. Yang, Applications of Pore-Expanded Mesoporous Silica. 1. Removal of Heavy Metal Cations and Organic Pollutants from Wastewater, *Chem. Mater.*, 2005, **17**(1), 212–216.

45 C. Wu, X. Huang, X. Wu, R. Qian and P. Jiang, Mechanically Flexible and Multifunctional Polymer-Based Graphene Foams for Elastic Conductors and Oil–Water Separators, *Adv. Mater.*, 2013, **25**(39), 5658–5662.

46 Y. Chu and Q. Pan, Three-Dimensionally Macroporous Fe/C Nanocomposites As Highly Selective Oil-Absorption Materials, *ACS Appl. Mater. Interfaces*, 2012, **4**(5), 2420–2425.

47 H. Liu and H. Qiu, Recent advances of 3D graphene-based adsorbents for sample preparation of water pollutants: a review, *Chem. Eng. J.*, 2020, **393**, 124691.

48 H. Bi, X. Xie, K. Yin, Y. Zhou, S. Wan and L. He, *et al.*, Spongy Graphene as a Highly Efficient and Recyclable Sorbent for Oils and Organic Solvents, *Adv. Funct. Mater.*, 2012, **22**(21), 4421–4425.

49 A. B. Dichiara, T. J. Sherwood, J. Benton-Smith, J. C. Wilson, S. J. Weinstein and R. E. Rogers, Free-standing carbon nanotube/graphene hybrid papers as next generation adsorbents, *Nanoscale*, 2014, **6**(12), 6322–6327.

50 X. Gui, J. Wei, K. Wang, A. Cao, H. Zhu and Y. Jia, *et al.*, Carbon nanotube sponges, *Adv. Mater.*, 2010, **22**(5), 617–621.

51 F. Hu, S. Chen, C. Wang, R. Yuan, D. Yuan and C. Wang, Study on the application of reduced graphene oxide and multiwall carbon nanotubes hybrid materials for simultaneous determination of catechol, hydroquinone, *p*-cresol and nitrite, *Anal. Chim. Acta*, 2012, **724**, 40–46.

52 C. P. Karan, R. Rengasamy and D. Das, *Oil spill cleanup by structured fibre assembly*. 2011.

53 S. Sabir, Approach of cost-effective adsorbents for oil removal from oily water, *Crit. Rev. Environ. Sci. Technol.*, 2015, **45**(17), 1916–1945.

54 S. Yang, L. Chen, L. Mu, B. Hao, J. Chen and P.-C. Ma, Graphene foam with hierarchical structures for the removal of organic pollutants from water, *RSC Adv.*, 2016, **6**(6), 4889–4898.

55 S. Yang, L. Chen, C. Wang, M. Rana and P.-C. Ma, Surface roughness induced superhydrophobicity of graphene foam for oil-water separation, *J. Colloid Interface Sci.*, 2017, **508**, 254–262.

56 Y. Qian, I. M. Ismail and A. Stein, Ultralight, high-surface-area, multifunctional graphene-based aerogels from self-assembly of graphene oxide and resol, *Carbon*, 2014, **68**, 221–231.

57 S. Stankovich, R. D. Piner, S. T. Nguyen and R. S. Ruoff, Synthesis and exfoliation of isocyanate-treated graphene oxide nanoplatelets, *Carbon*, 2006, **44**(15), 3342–3347.

58 S. Stankovich, D. A. Dikin, G. H. Dommett, K. M. Kohlhaas, E. J. Zimney and E. A. Stach, *et al.*, Graphene-based composite materials, *Nature*, 2006, **442**(7100), 282–286.

59 S. Park, J. An, I. Jung, R. D. Piner, S. J. An and X. Li, *et al.*, Colloidal suspensions of highly reduced graphene oxide in a wide variety of organic solvents, *Nano Lett.*, 2009, **9**(4), 1593–1597.

60 S. Stankovich, D. A. Dikin, R. D. Piner, K. A. Kohlhaas, A. Kleinhammes and Y. Jia, *et al.*, Synthesis of graphene-based nanosheets via chemical reduction of exfoliated graphite oxide, *Carbon*, 2007, **45**(7), 1558–1565.

61 H. He, T. Riedl, A. Lerf, J. Klinowski and N. M. R. Solid-state, studies of the structure of graphite oxide, *J. Phys. Chem.*, 1996, **100**(51), 19954–19958.

62 H. He, J. Klinowski, M. Forster and A. Lerf, A new structural model for graphite oxide, *Chem. Phys. Lett.*, 1998, **287**(1–2), 53–56.

63 A. Lerf, H. He, T. Riedl, M. Forster and J. Klinowski,  $^{13}\text{C}$  and  $^1\text{H}$  MAS NMR studies of graphite oxide and its chemically modified derivatives, *Solid State Ionics*, 1997, **101**, 857–862.

64 A. Lerf, H. He, M. Forster and J. Klinowski, Structure of graphite oxide revisited, *J. Phys. Chem. B*, 1998, **102**(23), 4477–4482.

65 A. B. Bourlinos, D. Gournis, D. Petridis, T. Szabó, A. Szeri and I. Dékány, Graphite oxide: chemical reduction to graphite and surface modification with primary aliphatic amines and amino acids, *Langmuir*, 2003, **19**(15), 6050–6055.

66 N. A. Kotov, I. Dékány and J. H. Fendler, Ultrathin graphite oxide-polyelectrolyte composites prepared by self-assembly: transition between conductive and non-conductive states, *Adv. Mater.*, 1996, **8**(8), 637–641.

67 Y. Zhao, C. Hu, Y. Hu, H. Cheng, G. Shi and L. Qu, A versatile, ultralight, nitrogen-doped graphene framework, *Angew. Chem., Int. Ed.*, 2012, **51**(45), 11371–11375.

68 H. Li, L. Liu and F. Yang, Covalent assembly of 3D graphene/polypyrrole foams for oil spill cleanup, *J. Mater. Chem. A*, 2013, **1**(10), 3446–3453.

69 H. Sun, Z. Xu and C. Gao, Multifunctional, ultra-flyweight, synergistically assembled carbon aerogels, *Adv. Mater.*, 2013, **25**(18), 2554–2560.

70 S. Kabiri, D. N. H. Tran, T. Altalhi and D. Losic, Outstanding adsorption performance of graphene–carbon nanotube aerogels for continuous oil removal, *Carbon*, 2014, **80**, 523–533.

71 N. Xiao, Y. Zhou, Z. Ling and J. Qiu, Synthesis of a carbon nanofiber/carbon foam composite from coal liquefaction residue for the separation of oil and water, *Carbon*, 2013, **59**, 530–536.

72 C.-F. Wang and S.-J. Lin, Robust superhydrophobic/superoleophilic sponge for effective continuous absorption and expulsion of oil pollutants from water, *ACS Appl. Mater. Interfaces*, 2013, **5**(18), 8861–8864.

73 S. Suni, A.-L. Kosunen, M. Hautala, A. Pasila and M. Romantschuk, Use of a by-product of peat excavation, cotton grass fibre, as a sorbent for oil-spills, *Mar. Pollut. Bull.*, 2004, **49**(11–12), 916–921.

74 M. Hussein, A. Amer and I. Sawsan, Oil spill sorption using carbonized pith bagasse: 1. Preparation and characterization of carbonized pith bagasse, *J. Anal. Appl. Pyrolysis*, 2008, **82**(2), 205–211.

75 W. Wan, R. Zhang, W. Li, H. Liu, Y. Lin and L. Li, *et al.*, Graphene–carbon nanotube aerogel as an ultra-light, compressible and recyclable highly efficient absorbent for oil and dyes, *Environ. Sci.: Nano*, 2016, **3**(1), 107–113.

76 C. Wang, S. Yang, Q. Ma, X. Jia and P.-C. Ma, Preparation of carbon nanotubes/graphene hybrid aerogel and its application for the adsorption of organic compounds, *Carbon*, 2017, **118**, 765–771.

77 W. Zhan, S. Yu, L. Gao, F. Wang, X. Fu and G. Sui, *et al.*, Bioinspired Assembly of Carbon Nanotube into Graphene Aerogel with “Cabbagelike” Hierarchical Porous Structure for Highly Efficient Organic Pollutants Cleanup, *ACS Appl. Mater. Interfaces*, 2018, **10**(1), 1093–1103.

78 T. Tao, G. Li, Y. He and P. Duan, Hybrid carbon nanotubes/graphene/nickel fluffy spheres for fast magnetic separation and efficient removal of organic solvents from water, *Mater. Lett.*, 2019, **254**, 440–443.

79 J. Cai, J. Tian, H. Gu and Z. Guo, Amino carbon nanotube modified reduced graphene oxide aerogel for oil/water separation, *ES Mater. Manuf.*, 2019, **6**(2), 68–74.

80 D. P. Hashim, N. T. Narayanan, J. M. Romo-Herrera, D. A. Cullen, M. G. Hahm and P. Lezzi, *et al.*, Covalently bonded three-dimensional carbon nanotube solids via boron induced nanojunctions, *Sci. Rep.*, 2012, **2**(1), 363.



81 L. Labiad and A. R. Kamali, 3D graphene nanoedges as efficient dye adsorbents with ultra-high thermal regeneration performance, *Appl. Surf. Sci.*, 2019, **490**, 383–394.

82 R. Nasiri and N. Arsalani, Synthesis and application of 3D graphene nanocomposite for the removal of cationic dyes from aqueous solutions: response surface methodology design, *J. Cleaner Prod.*, 2018, **190**, 63–71.

83 Y. Liu, Y. Tian, C. Luo, G. Cui and S. Yan, One-pot preparation of a  $\text{MnO}_2$ -graphene–carbon nanotube hybrid material for the removal of methyl orange from aqueous solutions, *New J. Chem.*, 2015, **39**(7), 5484–5492.

84 Z. Sui, Q. Meng, X. Zhang, R. Ma and B. Cao, Green synthesis of carbon nanotube–graphene hybrid aerogels and their use as versatile agents for water purification, *J. Mater. Chem.*, 2012, **22**(18), 8767.

85 S. K. Das, J. Bhowal, A. R. Das and A. K. Guha, Adsorption behavior of rhodamine B on *rhizopus oryzae* biomass, *Langmuir*, 2006, **22**(17), 7265–7272.

86 L. Sun, C. Tian, L. Wang, J. Zou, G. Mu and H. Fu, Magnetically separable porous graphitic carbon with large surface area as excellent adsorbents for metal ions and dye, *J. Mater. Chem.*, 2011, **21**(20), 7232–7239.

87 B. S. Girgis, A. M. Soliman and N. A. Fathy, Development of micro-mesoporous carbons from several seed hulls under varying conditions of activation, *Microporous Mesoporous Mater.*, 2011, **142**(2–3), 518–525.

88 L. Ai and J. Jiang, Removal of methylene blue from aqueous solution with self-assembled cylindrical graphene–carbon nanotube hybrid, *Chem. Eng. J.*, 2012, **192**, 156–163.

89 M. Kotal and A. K. Bhowmick, Multifunctional hybrid materials based on carbon nanotube chemically bonded to reduced graphene oxide, *J. Phys. Chem. C*, 2013, **117**(48), 25865–25875.

90 K. Goh, W. Jiang, H. E. Karahan, S. Zhai, L. Wei and D. Yu, *et al.*, All-carbon nanoarchitectures as high-performance separation membranes with superior stability, *Adv. Funct. Mater.*, 2015, **25**(47), 7348–7359.

91 B. Lee, S. Lee, M. Lee, D. H. Jeong, Y. Baek and J. Yoon, *et al.*, Carbon nanotube-bonded graphene hybrid aerogels and their application to water purification, *Nanoscale*, 2015, **7**(15), 6782–6789.

92 N. Li, M. Zheng, X. Chang, G. Ji, H. Lu and L. Xue, *et al.*, Preparation of magnetic  $\text{CoFe}_2\text{O}_4$ -functionalized graphene sheets *via* a facile hydrothermal method and their adsorption properties, *J. Solid State Chem.*, 2011, **184**(4), 953–958.

93 Y. Yao, S. Miao, S. Liu, L. P. Ma, H. Sun and S. Wang, Synthesis, characterization, and adsorption properties of magnetic  $\text{Fe}_3\text{O}_4$ @graphene nanocomposite, *Chem. Eng. J.*, 2012, **184**, 326–332.

94 X. Chen, M. Qiu, H. Ding, K. Fu and Y. Fan, A reduced graphene oxide nanofiltration membrane intercalated by well-dispersed carbon nanotubes for drinking water purification, *Nanoscale*, 2016, **8**(10), 5696–5705.

95 M. O. Ansari, R. Kumar, S. A. Ansari, S. P. Ansari, M. A. Barakat and A. Alshahri, *et al.*, Anion selective pTSA doped polyaniline@graphene oxide-multiwalled carbon nanotube composite for Cr(vi) and Congo red adsorption, *J. Colloid Interface Sci.*, 2017, **496**, 407–415.

96 Y. Huang, J. Zhu, H. Liu, Z. Wang and X. Zhang, Preparation of porous graphene/carbon nanotube composite and adsorption mechanism of methylene blue, *SN Appl. Sci.*, 2019, **1**(1), 37.

97 F. Yue, Q. Zhang, L. Xu, Y. Zheng, C. Yao and J. Jia, *et al.*, Porous Reduced Graphene Oxide/Single-Walled Carbon Nanotube Film as Freestanding and Flexible Electrode Materials for Electrosorption of Organic Dye, *ACS Appl. Nano Mater.*, 2019, **2**(10), 6258–6267.

98 S. Su, Y. Liu, W. He, X. Tang, W. Jin and Y. Zhao, A novel graphene oxide–carbon nanotubes anchored  $\alpha\text{-FeOOH}$  hybrid activated persulfate system for enhanced degradation of Orange II, *J. Environ. Sci.*, 2019, **83**, 73–84.

99 T. Yao, L. Qiao and K. Du, High tough and highly porous graphene/carbon nanotubes hybrid beads enhanced by carbonized polyacrylonitrile for efficient dyes adsorption, *Microporous Mesoporous Mater.*, 2020, **292**, 109716.

100 C. Hu, D. Grant, X. Hou and F. Xu, High rhodamine B and methyl orange removal performance of graphene oxide/carbon nanotube nanostructures, *Mater. Today Proc.*, 2020, S2214785320314772.

101 T. Liu, B. Gao, J. Fang, B. Wang and X. Cao, Biochar-supported carbon nanotube and graphene oxide nanocomposites for Pb(II) and Cd(II) removal, *RSC Adv.*, 2016, **6**(29), 24314–24319.

102 R. Nasiri, N. Arsalani and Y. Panahian, One-pot synthesis of novel magnetic three-dimensional graphene/chitosan/nickel ferrite nanocomposite for lead ions removal from aqueous solution: RSM modelling design, *J. Cleaner Prod.*, 2018, **201**, 507–515.

103 B. Tan, H. Zhao, Y. Zhang, X. Quan, Z. He and W. Zheng, *et al.*, Amphiphilic PA-induced three-dimensional graphene macrostructure with enhanced removal of heavy metal ions, *J. Colloid Interface Sci.*, 2018, **512**, 853–861.

104 S. Wang, H. Sun, H.-M. Ang and M. Tadé, Adsorptive remediation of environmental pollutants using novel graphene-based nanomaterials, *Chem. Eng. J.*, 2013, **226**, 336–347.

105 D. Zhao, Y. Wang, S. Zhao, M. Wakeel, Z. Wang and R. S. Shaikh, *et al.*, A simple method for preparing ultra-light graphene aerogel for rapid removal of U(VI) from aqueous solution, *Environ. Pollut.*, 2019, **251**, 547–554.

106 H. Gao, Y. Sun, J. Zhou, R. Xu and H. Duan, Mussel-inspired synthesis of polydopamine-functionalized graphene hydrogel as reusable adsorbents for water purification, *ACS Appl. Mater. Interfaces*, 2013, **5**(2), 425–432.

107 Y. Lei, F. Chen, Y. Luo and L. Zhang, Synthesis of three-dimensional graphene oxide foam for the removal of heavy metal ions, *Chem. Phys. Lett.*, 2014, **593**, 122–127.

108 X. Mi, G. Huang, W. Xie, W. Wang, Y. Liu and J. Gao, Preparation of graphene oxide aerogel and its adsorption for  $\text{Cu}^{2+}$  ions, *Carbon*, 2012, **50**(13), 4856–4864.

109 M. Liu, C. Chen, J. Hu, X. Wu and X. Wang, Synthesis of magnetite/graphene oxide composite and application for



cobalt(II) removal, *J. Phys. Chem. C*, 2011, **115**(51), 25234–25240.

110 G. Zhao, X. Ren, X. Gao, X. Tan, J. Li and C. Chen, *et al.*, Removal of Pb(II) ions from aqueous solutions on few-layered graphene oxide nanosheets, *Dalton Trans.*, 2011, **40**(41), 10945–10952.

111 N. Zhang, H. Qiu, Y. Si, W. Wang and J. Gao, Fabrication of highly porous biodegradable monoliths strengthened by graphene oxide and their adsorption of metal ions, *Carbon*, 2011, **49**(3), 827–837.

112 B. Xiao and K. Thomas, Competitive adsorption of aqueous metal ions on an oxidized nanoporous activated carbon, *Langmuir*, 2004, **20**(11), 4566–4578.

113 M. Benítez, D. Das, R. Ferreira, U. Pischel and H. García, Urea-containing mesoporous silica for the adsorption of Fe(III) cations, *Chem. Mater.*, 2006, **18**(23), 5597–5603.

114 A. Liu, K. Hidajat, S. Kawi and D. Zhao, A new class of hybrid mesoporous materials with functionalized organic monolayers for selective adsorption of heavy metal ions, *Chem. Commun.*, 2000, (13), 1145–1146.

115 L. Li, G. Zhou, Z. Weng, X.-Y. Shan, F. Li and H.-M. Cheng, Monolithic  $\text{Fe}_2\text{O}_3$ /graphene hybrid for highly efficient lithium storage and arsenic removal, *Carbon*, 2014, **67**, 500–507.

116 M. Zhang, B. Gao, X. Cao and L. Yang, Synthesis of a multifunctional graphene–carbon nanotube aerogel and its strong adsorption of lead from aqueous solution, *RSC Adv.*, 2013, **3**(43), 21099–21105.

117 S. Vadahanambi, S.-H. Lee, W.-J. Kim and I.-K. Oh, Arsenic removal from contaminated water using three-dimensional graphene–carbon nanotube–iron oxide nanosstructures, *Environ. Sci. Technol.*, 2013, **47**(18), 10510–10517.

118 B. P. Viraka Nellore, R. Kanchanapally, F. Pedraza, S. S. Sinha, A. Pramanik and A. T. Hamme, *et al.*, Bio-conjugated CNT-bridged 3D porous graphene oxide membrane for highly efficient disinfection of pathogenic bacteria and removal of toxic metals from water, *ACS Appl. Mater. Interfaces*, 2015, **7**(34), 19210–19218.

119 Z. Gu, Y. Wang, J. Tang, J. Yang, J. Liao and Y. Yang, *et al.*, The removal of uranium(VI) from aqueous solution by graphene oxide–carbon nanotubes hybrid aerogels, *J. Radioanal. Nucl. Chem.*, 2015, **303**(3), 1835–1842.

120 X. Zhu, Y. Cui, X. Chang and H. Wang, Selective solid-phase extraction and analysis of trace-level Cr(III), Fe(III), Pb(II), and Mn(II) Ions in wastewater using diethylenetriamine-functionalized carbon nanotubes dispersed in graphene oxide colloids, *Talanta*, 2016, **146**, 358–363.

121 L. Guo, Y. Xu, M. Zhuo, L. Liu, Q. Xu and L. Wang, *et al.*, Highly efficient removal of Gd(III) using hybrid hydrogels of carbon nanotubes/graphene oxide in dialysis bags and synergistic enhancement effect, *Chem. Eng. J.*, 2018, **348**, 535–545.

122 W. Zhan, L. Gao, X. Fu, S. H. Siyal, G. Sui and X. Yang, Green synthesis of amino-functionalized carbon nanotube–graphene hybrid aerogels for high performance heavy metal ions removal, *Appl. Surf. Sci.*, 2019, **467**, 1122–1133.

123 A. Ghozatloo and M. Shariaty-Niassar, Graphene/CNT hybrid effect on Absorption of Mn<sup>2+</sup> by Activated Carbon, *Anal. Methods Environ. Chem.*, 2019, **2**(2), 31–36.

124 H. Huang, T. Chen, X. Liu and H. Ma, Ultrasensitive and simultaneous detection of heavy metal ions based on three-dimensional graphene–carbon nanotubes hybrid electrode materials, *Anal. Chim. Acta*, 2014, **852**, 45–54.

125 F. Yang, D. He, B. Zheng, D. Xiao, L. Wu and Y. Guo, Self-assembled hybrids with xanthate functionalized carbon nanotubes and electro-exfoliating graphene sheets for electrochemical sensing of copper ions, *J. Electroanal. Chem.*, 2016, **767**, 100–107.

126 P. N. D. Duoc, N. H. Binh, T. V. Hau, C. T. Thanh, P. V. Trinh and N. V. Tuyen, *et al.*, A novel electrochemical sensor based on double-walled carbon nanotubes and graphene hybrid thin film for arsenic(V) detection, *J. Hazard. Mater.*, 2020, **400**, 123185.

127 T. AL-Gahouari, G. Bodkhe, P. Sayyad, N. Ingle, M. Mahadik and S. M. Shirsat, *et al.*, Electrochemical Sensor: L-Cysteine Induced Selectivity Enhancement of Electrochemically Reduced Graphene Oxide–Multiwalled Carbon Nanotubes Hybrid for Detection of Lead (Pb<sup>2+</sup>) Ions, *Front. Mater.*, 2020, **7**, 68.

128 J. Kong, N. R. Franklin, C. Zhou, M. G. Chapline, S. Peng and K. Cho, *et al.*, Nanotube molecular wires as chemical sensors, *Science*, 2000, **287**(5453), 622–625.

129 Q. Wan, Q. Li, Y. Chen, T.-H. Wang, X. He and J. Li, *et al.*, Fabrication and ethanol sensing characteristics of ZnO nanowire gas sensors, *Appl. Phys. Lett.*, 2004, **84**(18), 3654–3656.

130 F. Schedin, A. K. Geim, S. V. Morozov, E. Hill, P. Blake and M. Katsnelson, *et al.*, Detection of individual gas molecules adsorbed on graphene, *Nat. Mater.*, 2007, **6**(9), 652–655.

131 J. D. Fowler, M. J. Allen, V. C. Tung, Y. Yang, R. B. Kaner and B. H. Weiller, Practical chemical sensors from chemically derived graphene, *ACS Nano*, 2009, **3**(2), 301–306.

132 G. Lu, L. E. Ocola and J. Chen, Reduced graphene oxide for room-temperature gas sensors, *Nanotechnology*, 2009, **20**(44), 445502.

133 T. Zhang, S. Mubeen, N. V. Myung and M. A. Deshusses, Recent progress in carbon nanotube-based gas sensors, *Nanotechnology*, 2008, **19**(33), 332001.

134 H. Y. Jeong, D.-S. Lee, H. K. Choi, D. H. Lee, J.-E. Kim and J. Y. Lee, *et al.*, Flexible room-temperature NO<sub>2</sub> gas sensors based on carbon nanotubes/reduced graphene hybrid films, *Appl. Phys. Lett.*, 2010, **96**(21), 213105.

135 A. Kaniyoor and S. Ramaprabhu, Hybrid carbon nanostructured ensembles as chemiresistive hydrogen gas sensors, *Carbon*, 2011, **49**(1), 227–236.

136 X. Dong, Y. Ma, G. Zhu, Y. Huang, J. Wang and M. B. Chan-Park, *et al.*, Synthesis of graphene–carbon nanotube hybrid foam and its use as a novel three-dimensional electrode for electrochemical sensing, *J. Mater. Chem.*, 2012, **22**(33), 17044–17048.

137 S. Liu, B. Yu, H. Zhang, T. Fei and T. Zhang, Enhancing NO<sub>2</sub> gas sensing performances at room temperature based

on reduced graphene oxide-ZnO nanoparticles hybrids, *Sens. Actuators, B*, 2014, **202**, 272–278.

138 W. Yuan, A. Liu, L. Huang, C. Li and G. Shi, High-performance NO<sub>2</sub> sensors based on chemically modified graphene, *Adv. Mater.*, 2013, **25**(5), 766–771.

139 S.-J. Choi, B.-H. Jang, S.-J. Lee, B. K. Min, A. Rothschild and I.-D. Kim, Selective detection of acetone and hydrogen sulfide for the diagnosis of diabetes and halitosis using SnO<sub>2</sub> nanofibers functionalized with reduced graphene oxide nanosheets, *ACS Appl. Mater. Interfaces*, 2014, **6**(4), 2588–2597.

140 C. Marichy, P. A. Russo, M. Latino, J.-P. Tessonniere, M.-G. Willinger and N. Donato, *et al.*, Tin dioxide–carbon heterostructures applied to gas sensing: structure-dependent properties and general sensing mechanism, *J. Phys. Chem. C*, 2013, **117**(38), 19729–19739.

141 G. Neri, S. G. Leonardi, M. Latino, N. Donato, S. Baek and D. E. Conte, *et al.*, Sensing behavior of SnO<sub>2</sub>/reduced graphene oxide nanocomposites toward NO<sub>2</sub>, *Sens. Actuators, B*, 2013, **179**, 61–68.

142 Z. Zhang, R. Zou, G. Song, L. Yu, Z. Chen and J. Hu, Highly aligned SnO<sub>2</sub> nanorods on graphene sheets for gas sensors, *J. Mater. Chem.*, 2011, **21**(43), 17360–17365.

143 Q. Lin, Y. Li and M. Yang, Tin oxide/graphene composite fabricated via a hydrothermal method for gas sensors working at room temperature, *Sens. Actuators, B*, 2012, **173**, 139–147.

144 S. Mao, S. Cui, G. Lu, K. Yu, Z. Wen and J. Chen, Tuning gas-sensing properties of reduced graphene oxide using tin oxide nanocrystals, *J. Mater. Chem.*, 2012, **22**(22), 11009–11013.

145 P. A. Russo, N. Donato, S. G. Leonardi, S. Baek, D. E. Conte and G. Neri, *et al.*, Room-temperature hydrogen sensing with heteronanostructures based on reduced graphene oxide and tin oxide, *Angew. Chem., Int. Ed.*, 2012, **51**(44), 11053–11057.

146 S. Liu, Z. Wang, Y. Zhang, C. Zhang and T. Zhang, High performance room temperature NO<sub>2</sub> sensors based on reduced graphene oxide-multiwalled carbon nanotubes–tin oxide nanoparticles hybrids, *Sens. Actuators, B*, 2015, **211**, 318–324.

147 T. T. Tung, C. Pham-Huu, I. Janowska, T. Kim, M. Castro and J.-F. Feller, Hybrid Films of Graphene and Carbon Nanotubes for High Performance Chemical and Temperature Sensing Applications, *Small*, 2015, **11**(28), 3485–3493.

148 S. K. Mishra, S. N. Tripathi, V. Choudhary and B. D. Gupta, Surface Plasmon Resonance-Based Fiber Optic Methane Gas Sensor Utilizing Graphene-Carbon Nanotubes–Poly(Methyl Methacrylate) Hybrid Nanocomposite, *Plasmonics*, 2015, **10**(5), 1147–1157.

149 A. Bisht, S. Chockalingam, O. Panwar, A. Kesarwani, B. Singh and V. Singh, Structural, field emission and ammonia gas sensing properties of multiwalled carbon nanotube-graphene like hybrid films deposited by microwave plasma enhanced chemical vapor deposition technique, *Sci. Adv. Mater.*, 2015, **7**(7), 1424–1434.

150 U. Yaqoob, A. I. Uddin and G.-S. Chung, A high-performance flexible NO<sub>2</sub> sensor based on WO<sub>3</sub> NPs decorated on MWCNTs and RGO hybrids on PI/PET substrates, *Sens. Actuators, B*, 2016, **224**, 738–746.

151 S.-J. Li, J.-C. Zhang, J. Li, H.-Y. Yang, J.-J. Meng and B. Zhang, A 3D sandwich structured hybrid of gold nanoparticles decorated MnO<sub>2</sub>/graphene-carbon nanotubes as high performance H<sub>2</sub>O<sub>2</sub> sensors, *Sens. Actuators, B*, 2018, **260**, 1–11.

152 Y. Seechaew, A. Wisitsoraat, D. Phokharatkul and C. Wongchoosuk, Room temperature toluene gas sensor based on TiO<sub>2</sub> nanoparticles decorated 3D graphene-carbon nanotube nanostructures, *Sens. Actuators, B*, 2019, **279**, 69–78.

153 Y. Seechaew, W. Pon-On and C. Wongchoosuk, Ultrahigh selective room-temperature ammonia gas sensor based on tin–titanium dioxide/reduced graphene/carbon nanotube nanocomposites by the solvothermal method, *ACS Omega*, 2019, **4**(16), 16916–16924.

154 S. Pyo, J. Choi and J. Kim, A Fully Transparent, Flexible, Sensitive, and Visible-Blind Ultraviolet Sensor Based on Carbon Nanotube-Graphene Hybrid, *Adv. Electron. Mater.*, 2019, **5**(2), 1800737.

155 F. Ghasemi, Vertically aligned carbon nanotubes, MoS<sub>2</sub>–rGo based optoelectronic hybrids for NO<sub>2</sub> gas sensing, *Sci. Rep.*, 2020, **10**(1), 11306.

156 P. M. Sudeep, T. N. Narayanan, A. Ganesan, M. M. Shajumon, H. Yang and S. Ozden, *et al.*, Covalently interconnected three-dimensional graphene oxide solids, *ACS Nano*, 2013, **7**(8), 7034–7040.

157 Z.-Y. Sui, Y. Cui, J.-H. Zhu and B.-H. Han, Preparation of three-dimensional graphene oxide–polyethylenimine porous materials as dye and gas adsorbents, *ACS Appl. Mater. Interfaces*, 2013, **5**(18), 9172–9179.

158 Y. He, N. Zhang, F. Wu, F. Xu, Y. Liu and J. Gao, Graphene oxide foams and their excellent adsorption ability for acetone gas, *Mater. Res. Bull.*, 2013, **48**(9), 3553–3558.

159 J. Liang, Z. Cai, L. Li, L. Guo and J. Geng, Scalable and facile preparation of graphene aerogel for air purification, *RSC Adv.*, 2014, **4**(10), 4843–4847.

160 M. De Marco, R. Menzel, S. M. Bawaked, M. Mokhtar, A. Y. Obaid and S. N. Basahel, *et al.*, Hybrid effects in graphene oxide/carbon nanotube-supported layered double hydroxides: enhancing the CO<sub>2</sub> sorption properties, *Carbon*, 2017, **123**, 616–627.

161 L. Wu, Z. Qin, L. Zhang, T. Meng, F. Yu and J. Ma, CNT-enhanced amino-functionalized graphene aerogel adsorbent for highly efficient removal of formaldehyde, *New J. Chem.*, 2017, **41**(7), 2527–2533.

162 B. Bhaduri, M. Engel, T. Polubesova, W. Wu, B. Xing and B. Chefetz, Dual functionality of an Ag–Fe<sub>3</sub>O<sub>4</sub>-carbon nanotube composite material: Catalytic reduction and antibacterial activity, *J. Environ. Chem. Eng.*, 2018, **6**(4), 4103–4113.

163 U. Szewzyk, R. Szewzyk, W. Manz and K.-H. Schleifer, Microbiological Safety of Drinking Water, *Annu. Rev. Microbiol.*, 2000, **54**(1), 81–127.

164 L. L. Zhang, Z. Xiong and X. Zhao, Pillaring chemically exfoliated graphene oxide with carbon nanotubes for photocatalytic degradation of dyes under visible light irradiation, *ACS Nano*, 2010, **4**(11), 7030–7036.

165 B. Zeng, X. Chen, X. Ning, C. Chen, W. Deng and Q. Huang, *et al.*, Electrostatic-assembly three-dimensional CNTs/rGO implanted Cu<sub>2</sub>O composite spheres and its photocatalytic properties, *Appl. Surf. Sci.*, 2013, **276**, 482–486.

166 C. Wang, M. Cao, P. Wang, Y. Ao, J. Hou and J. Qian, Preparation of graphene–carbon nanotube-TiO<sub>2</sub> composites with enhanced photocatalytic activity for the removal of dye and Cr(vi), *Appl. Catal., A*, 2014, **473**, 83–89.

167 L. Zhang, H. Li, Y. Liu, Z. Tian, B. Yang and Z. Sun, *et al.*, Adsorption-photocatalytic degradation of methyl orange over a facile one-step hydrothermally synthesized TiO<sub>2</sub>/ZnO-NH<sub>2</sub>-RGO nanocomposite, *RSC Adv.*, 2014, **4**(89), 48703–48711.

168 N. A. Fathy, S. E. El-Shafey, O. I. El-Shafey and W. S. Mohamed, Oxidative degradation of RB19 dye by a novel  $\gamma$ -MnO<sub>2</sub>/MWCNT nanocomposite catalyst with H<sub>2</sub>O<sub>2</sub>, *J. Environ. Chem. Eng.*, 2013, **1**(4), 858–864.

169 N. A. Fathy, S. M. El-Khouly, N. A. Hassan and R. M. Awad, Free-and Ni-doped carbon xerogels catalysts for wet peroxide oxidation of methyl orange, *J. Water Process Eng.*, 2017, **16**, 21–27.

170 R. S. Ribeiro, N. A. Fathy, A. A. Attia, A. M. Silva, J. L. Faria and H. T. Gomes, Activated carbon xerogels for the removal of the anionic azo dyes Orange II and Chromotrope 2R by adsorption and catalytic wet peroxide oxidation, *Chem. Eng. J.*, 2012, **195**, 112–121.

171 N. A. Fathy, S. E. El-Shafey and O. I. El-Shafey, Synthesis of a novel MnO<sub>2</sub> @carbon nanotubes-graphene hybrid catalyst (MnO<sub>2</sub>@CNT-G) for catalytic oxidation of basic red 18 dye (BR18), *J. Water Process Eng.*, 2017, **17**, 95–101.

172 H. Wang, S. Li, Y. Si, Z. Sun, S. Li and Y. Lin, Recyclable enzyme mimic of cubic Fe<sub>3</sub>O<sub>4</sub> nanoparticles loaded on graphene oxide-dispersed carbon nanotubes with enhanced peroxidase-like catalysis and electrocatalysis, *J. Mater. Chem. B*, 2014, **2**(28), 4442–4448.

173 Y. Liu, X. Liu, Y. Zhao and D. D. Dionysiou, Aligned  $\alpha$ -FeOOH nanorods anchored on a graphene oxide–carbon nanotubes aerogel can serve as an effective Fenton-like oxidation catalyst, *Appl. Catal., B*, 2017, **213**, 74–86.

174 L. Qu, G. Zhu, J. Ji, T. Yadav, Y. Chen and G. Yang, *et al.*, Recyclable visible light-driven O<sub>2</sub>-C<sub>3</sub>N<sub>4</sub>/graphene oxide/N-carbon nanotube membrane for efficient removal of organic pollutants, *ACS Appl. Mater. Interfaces*, 2018, **10**(49), 42427–42435.

175 G. Yi, Z. Chang, G. Liu and L. Yang, *In situ* fabrication of copper nanocubes with platinum skin on 3D graphene–carbon nanotubes hybrid for efficient methanol electrooxidation, *Int. J. Electrochem. Sci.*, 2019, **14**, 7232–7240.

176 Z. Mohammadi and M. H. Entezari, Sono-synthesis approach in uniform loading of ultrafine Ag nanoparticles on reduced graphene oxide nanosheets: an efficient catalyst for the reduction of 4-nitrophenol, *Ultrason. Sonochem.*, 2018, **44**, 1–13.

177 Z. Yan, L. Fu, X. Zuo and H. Yang, Green assembly of stable and uniform silver nanoparticles on 2D silica nanosheets for catalytic reduction of 4-nitrophenol, *Appl. Catal., B*, 2018, **226**, 23–30.

178 K. Zhu, C. Chen, S. Lu, X. Zhang, A. Alsaedi and T. Hayat, MOFs-induced encapsulation of ultrafine Ni nanoparticles into 3D N-doped graphene–CNT frameworks as a recyclable catalyst for Cr(vi) reduction with formic acid, *Carbon*, 2019, **148**, 52–63.

179 X. T. Tran, M. Hussain and H. T. Kim, Facile and fast synthesis of a reduced graphene oxide/carbon nanotube/iron/silver hybrid and its enhanced performance in catalytic reduction of 4-nitrophenol, *Solid State Sci.*, 2020, **100**, 106107.

180 J. Liang, Z. Ding, H. Qin, J. Li, W. Wang and D. Luo, *et al.*, Ultra-fast enrichment and reduction of As(v)/Se(vi) on three dimensional graphene oxide sheets-oxidized carbon nanotubes hydrogels, *Environ. Pollut.*, 2019, **251**, 945–951.

181 M. R. Islam, M. Ferdous, M. I. Sujan, X. Mao, H. Zeng and M. S. Azam, Recyclable Ag-decorated highly carbonaceous magnetic nanocomposites for the removal of organic pollutants, *J. Colloid Interface Sci.*, 2020, **562**, 52–62.

182 M. Kotal, A. Sharma, S. Jakhar, V. Mishra, S. Roy and S. C. Sahoo, *et al.*, Graphene-Templated Cobalt Nanoparticle Embedded Nitrogen-Doped Carbon Nanotubes for Efficient Visible-Light Photocatalysis, *Cryst. Growth Des.*, 2020, **20**(7), 4627–4639.

183 F. Field and J. R. Ehrenfeld, Life-cycle analysis: the role of evaluation and strategy, *Meas. Environ. Perform. Ecosyst. Cond.*, 1999, 29–41.

184 A. B. Dichiara, S. J. Weinstein and R. E. Rogers, On the choice of batch or fixed bed adsorption processes for wastewater treatment, *Ind. Eng. Chem. Res.*, 2015, **54**(34), 8579–8586.

185 X. T. Liu, X. Y. Mu, X. L. Wu, L. X. Meng, W. B. Guan and Y. Qiang, *et al.*, Toxicity of multi-walled carbon nanotubes, graphene oxide, and reduced graphene oxide to zebrafish embryos, *Biomed. Environ. Sci.*, 2014, **27**(9), 676–683.

186 R. Das, S. B. Abd Hamid, M. E. Ali, A. F. Ismail, M. Annuar and S. Ramakrishna, Multifunctional carbon nanotubes in water treatment: the present, past and future, *Desalination*, 2014, **354**, 160–179.

187 C.-J. Shih, S. Lin, R. Sharma, M. S. Strano and D. Blankschtein, Understanding the pH-dependent behavior of graphene oxide aqueous solutions: a comparative experimental and molecular dynamics simulation study, *Langmuir*, 2012, **28**(1), 235–241.

188 S. Kashyap, S. Mishra and S. K. Behera, Aqueous colloidal stability of graphene oxide and chemically converted graphene, *J. Nanoparticles*, 2014, **2014**, 640281.

189 J. Zhao, Z. Wang, J. C. White and B. Xing, Graphene in the aquatic environment: adsorption, dispersion, toxicity and transformation, *Environ. Sci. Technol.*, 2014, **48**(17), 9995–10009.